

報告番号 P 第 831 号

TUNNELING SPECTROSCOPY  
OF  
IMPURITY BAND

NOBUHIKO SAWAKI

## CONTENTS

I.	Introduction	Page
1-1	Basic Concepts of Tunneling in Solids .....	1
1-2	Heavily Doped Semiconductors .....	5
1-3	Tunneling Spectroscopic Study of Impurity Band ( Purpose of the Research ) .....	8
II.	Tunneling and Density of States	
2-1	Basic Formulation of Tunneling .....	10
2-2	Tunneling Probability for a p-n junction .....	14
2-3	Current Formula and Density of States .....	25
III.	Tunneling into Impurity Band ( I ) ( One Electron Approximation )	
3-1	One Electron Wave Function .....	29
3-2	Current Formula and Density of States .....	36
3-3	Experimental Investigation of Density of States .....	40
3-4	Notes on the Quasi-particle Approximation .....	45
IV.	Tunneling into Impurity Band ( II ) ( Self-energy Effect )	
4-1	Formulation of the Problem .....	48
4-2	Current Formula for Short Range Potential .....	53
4-3	Numerical Investigation of the Conductance .....	60
4-4	Experimental Considerations .....	67
V.	Localization and Density of States	
5-1	Magnetic Moment in Tunnel Diode .....	73
5-2	Experimentals .....	75
5-3	Localized Spin and Density of States .....	80
VI.	Summary .....	82
	Acknowledgements .....	84
	References .....	85
	List of Reports .....	93

## I. INTRODUCTION

### § 1 - 1 Basic Concepts of Tunneling in Solids ( Historical Survey )

The concepts of tunneling, which are purely a quantum mechanical process, that a particle passes from a classically allowed region to another allowed region through a potential barrier (Fig.1-1) was first utilized by Oppenheimer<sup>1)</sup> to the autoionization of hydrogen atom in an electric field. After that such phenomena as  $\alpha$ -decay of a heavy nucleus<sup>2)</sup> and Zener breakdown of an insulator<sup>3)</sup> have been understood by the tunneling process.

Earlier the Zener model of tunneling was adopted to the breakdown of a p-n diode and verified the current-voltage characteristics qualitatively.<sup>4)</sup> But the most convincing experimental evidence of the tunneling in a p-n junction was given by the invention of a tunnel diode by Esaki.<sup>5)</sup> He discovered that a narrow p-n junction, illustrated in Fig.1-2, of which concentration of donors and acceptors are sufficiently high exhibits a negative resistance, and found that the I-V characteristics are well interpreted by the tunneling model, proposing phenomenologically a formula called Esaki Integral;

$$J = \int Z_{p-n} \rho_p \rho_n (f_p - f_n) dE, \quad (1-1)$$

where  $\rho_n$  and  $\rho_p$  are the density of states of electrons and holes, respectively,  $f_n$ ,  $f_p$  the Fermi-Dirac distribution function and  $Z_{p-n}$  is the tunneling probability. Following Esaki's original analysis, the theory of tunneling in a p-n junction was developed by many authors, e.g. Kane,<sup>6)</sup> Keldysh,<sup>7)</sup> Harrison,<sup>8)</sup> Fredkin and Wannier,<sup>9)</sup> Moll<sup>10)</sup> and etc. They obtained a similar formula described as

$$J = \int P_{p-n} (f_p - f_n) dE \int dE_{\perp}, \quad (1-2)$$

where the tunneling probability  $P_{p-n}$  is given by applying the WKB method<sup>11)</sup>

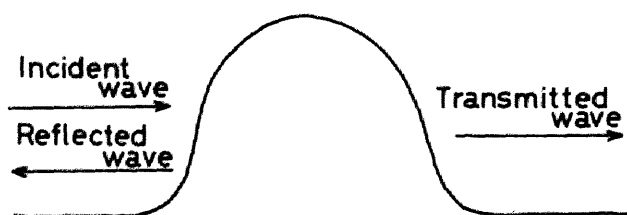


Fig. 1-1. Basic concepts of tunneling

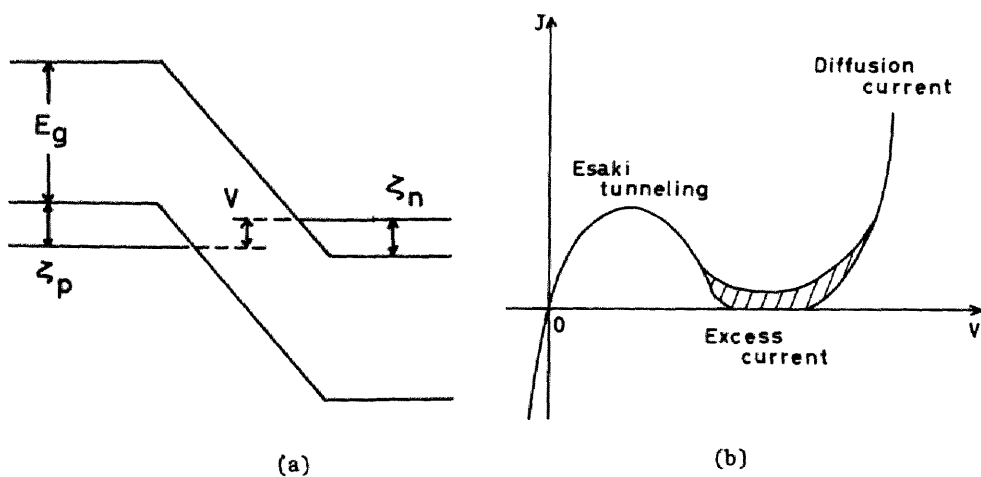


Fig. 1-2. (a) Schematic energy diagram of the narrow p-n junction invented by Esaki. (b) Current-voltage characteristics of Esaki diode.

to the uniform-field junction in three dimensions as

$$P_{p-n} = \exp(-E_g/4\bar{E}_L) \exp(-E_L/\bar{E}_L) \quad , \quad (1-3)$$

$$\bar{E}_L = \sqrt{2} \hbar F / 2 \pi (m^* E_g)^{\frac{1}{2}} \quad . \quad (1-4)$$

Equation (1-3) differs only in the last factor, which describes the energy component parallel to the junction plane, from the one dimensional model.<sup>11)</sup> In spite of the doubtfulness of the WKB approximation for a state of long wave length<sup>12)</sup> ( which seems especially important in the case of a semiconductor junction because of its smaller Fermi degeneracy ), following several years were devoted to investigate the current-voltage characteristics of various kinds of junctions by applying the formula given by Eqs.(1-2) - (1-4), and many fruitful results have been obtained.<sup>13-16)</sup>

In the earlier stage of the studies the interest was stimulated to the direct band to band transitions. In 1959, however, Holonyak et al.<sup>17)</sup> observed sharp thresholds in the I-V characteristics of a Si tunnel diode corresponding to the onset of phonon emission, and excited interest in the indirect interband transition.<sup>18-21)</sup> The impurity induced tunneling transition was also observed<sup>22)</sup> and some theoretical investigation have been done.<sup>23,24)</sup> But we have not obtained full understanding of the phenomena as yet.

The year 1966 was full of topics and the history of tunneling took a new turn. Esaki<sup>25)</sup> observed another thresholds in the current-voltage characteristics due to energy band structures of material and determined the band energies of Bi, proving that tunneling is a powerful method to study the energy band structures of semiconductors and semimetals. Conley, Duke, Mahan and Tiemann<sup>26)</sup> investigated the incremental resistance of a Schottky tunnel junction and determined experimentally the Fermi energy. Two of them ( Conley-Mahan<sup>27)</sup> and Mahan-Conley<sup>28)</sup> ) studied a GaAs Schottky junction and showed a possibility to determine the density of states by tunneling.<sup>29)</sup>

The theory of magnetic scattering ( Kondo effect ) in a tunnel diode was proposed by Anderson<sup>30)</sup> and Appelbaum,<sup>31,32)</sup> which was later developed to the many body theory in tunneling.<sup>33)</sup> The experimental evidence of the many body effect was found by Hall et al.<sup>34)</sup> They observed a temperature sensitive conductance dip around zero-bias called zero-bias conductance anomaly (ZBA) in a p-n junction made of III-V compound semicon-

ductors. The ZBA have been observed in almost all kind of tunnel junction at low temperatures ( usually at liq.He temperature ), and several causes of the phenomena have been proposed; (1) magnetic scattering<sup>35,36)</sup> (2) collective excitations of phonons<sup>37)</sup> (3) defects<sup>38,39)</sup> (4) superconductors.<sup>40)</sup> Duke<sup>41)</sup> developed an unified theory of tunneling including ZBA by making use of Kubo's linear response formalism,<sup>42)</sup> and got an expression for tunneling between many body states of the form

$$J = \frac{2e}{\hbar} \text{Im} \sum \Lambda_{k_1 q_1} \Lambda_{k_2 q_2}^\dagger \langle T_\tau [c_{k_1 \alpha_1}^\dagger(\tau) c_{q_1 \alpha_1}(\tau) c_{q_2 \alpha_2}^\dagger(\tau') c_{k_2 \alpha_2}(\tau')] \rangle, \quad (1-5)$$

where  $\Lambda_{kq}$  is the vertex function,  $T_\tau$  the Wick's chronological operator and  $c^\dagger$  and  $c$  are respectively the temperature dependent creation and annihilation operator. This formula contains the many body density of states factor through the temperature Green function given by<sup>43)</sup>

$$G(\tau - \tau') = \langle T_\tau [c_{k\alpha}(\tau) c_{k\alpha}^\dagger(\tau')] \rangle \quad (1-6)$$

By using Eq.(1-5) several interactions of tunneling electrons have been verified, e.g. phonons,<sup>37,44)</sup> plasmons,<sup>45)</sup> and several excitations in superconductors.<sup>46)</sup> Thus tunneling has been proved to be a powerful probe of the elementary excitations in semiconductors as well as a measure of the correctness of the many body theory.

Besides the developments of tunneling in semiconductors, the works about superconductors must be remembered. Following the original observations of the BCS gap by Gieaver<sup>40)</sup> in a tunneling junction made of Pb, the theory of tunneling in a superconductor was established by Bardeen<sup>47)</sup> and Cohen et al.<sup>48)</sup> To date extensive studies of this field of spectroscopy have done and such properties as gapless superconductor and Josephson effects have been studied with tunneling.<sup>49,50)</sup> It must be born in mind that the theory of tunneling from a many particle point of view described above was originally established for the description of tunneling in superconductors.

## § 1 - 2      Heavily Doped Semiconductors

Contrary to the efforts in semiconductor material science to make it as pure as possible, the interest in the effects of heavily doping on the electronic properties has been stimulated by the tunnel diode physics.

By increasing the degree of doping the average distance between the impurities decreases and these atoms begin to interact or the wave functions of electrons localized at each atoms begin to overlap. The energy level of donors ( or acceptors ) is broadened to form an impurity band.<sup>51)</sup> The electrons are then easy to travel from site to site responsible for the electrical conductivity and simple localized picture of impurity state becomes doubtful.<sup>52)</sup> If the concentration is increased further the band width of the impurity band may become broader and finally merges into the conduction ( or valence ) band.<sup>53)</sup> The introduction of the impurity atoms breaks the periodicity of the crystal and the van Hove singularity at the band edge<sup>54)</sup> will disappear, helping the merging of the impurity band. In this highly doped material the impurity potential is expected to become weaker by the screening effect due to many charge carriers.<sup>54,55)</sup> Thus we cannot distinguish an electron bounded to an impurity atom from conduction electrons, and electrons are well approximated by the free electron description or the sample is in the metallic region of concentration. The material of this highly doping is called heavily doped or degenerate,<sup>56)</sup> We must use the Fermi-Dirac statistics for electrons and holes. Tunnel diode is available by making use of this heavily doped semiconductor and the band tail ( or the impurity band ) is thought to be at least partially responsible for valley and excess current.<sup>57,58)</sup>

In a standard theory of semiconductors the properties of an electron in the conduction band are often approximated by a plane wave with the effective mass, and donor states by the hydrogen atom 1S state.<sup>59,60)</sup> In a heavily doped semiconductor, however, the large number of donor impurities can supply many electrons in the conduction band. Therefore the system contains many interactions, i.e. electron-electron, electron-impurity and impurity-impurity interaction as well as electron-lattice interaction.<sup>54,61)</sup> To make the problem more complicated, the impurity atoms are thought to distribute utterly at random in the whole crystal, which makes the exact treatment of the interactions impossible. We can know the physical properties only through the statistical averages.<sup>62)</sup>

The principle of the coherent potential approximation ( CPA ) is to reduce those interaction energies into the electronic self-energy and in this scheme we can see an electron traveling in the statistically averaged potential.<sup>63)</sup> Thus though the interest in the heavily doped semiconductors was stimulated by the invention of a tunnel diode, they are of interest from a broader point of view, i.e. the problem in the heavily doped material is that of many body problem and it serves us a good example of the general problem of the energy spectra of a disordered system, which had been earlier studied as the phonon spectra of random lattice.<sup>64)</sup>

In the past ten years, many works have been published on how to take into account properly the disorderness as well as the many body aspects and much of the electronic and electrical properties associated with the impurity band have been resolved, e.g. density of states, electron mobility, magnetic susceptibility and Hall coefficient.<sup>65-71)</sup> They showed that almost all of the properties are closely related to the electron density of states, which is sensitive to what model is used for the individual impurity potential and to what interactions are taken into account.

Since the observation of the impurity conduction in a germanium single crystal by Fritzsche<sup>72)</sup> various phenomena have been studied,<sup>73-75)</sup> one of the most interesting of which is the negative magneto-resistance.<sup>76)</sup> The phenomena are very similar to Kondo effect in a dilute magnetic alloy<sup>77)</sup> and attributed to the localized magnetic moment due to electron correlation in a random lattice.<sup>78)</sup> It has been thought as a true effect that the impurity band really exists and there have been some evidences of the effect.<sup>79,80)</sup> But the density of states has not yet been measured as a function of energy and we don't know whether the band tail (impurity band ) decays continuously into the forbidden band<sup>81)</sup> or it has any cut-off.<sup>68)</sup> Such a principle question is still controversial if an impurity band ever exists separated from the main band.<sup>82)</sup>

The concepts of the mobility gap in an amorphous semiconductor,<sup>83)</sup> which is an ideal random lattice, presented a question if electron is localized in a continuous energy spectrum. The band tail in a heavily doped semiconductor has been exposed to similar question,<sup>84)</sup> and the problem of the duality of the localization and delocalization in these states has given us an academic problem as well as a practical problem.<sup>85)</sup>



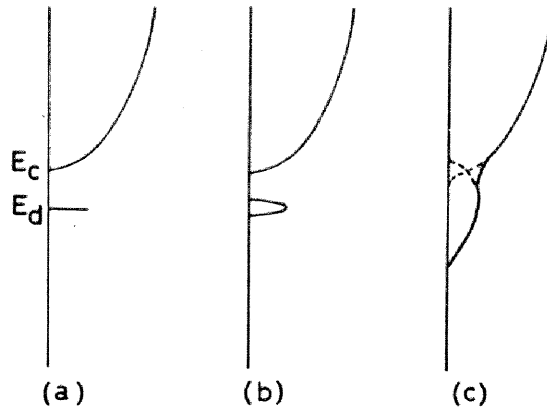


Fig. 1-3. Density of states of a doped semiconductor. (a) At low concentration a donor level is formed below the conduction band minimum. (b) By increasing the concentration the donor level is broadened by the overlapping of the wave functions. (c) In the metallic concentration region, the impurity band merges into the main band.

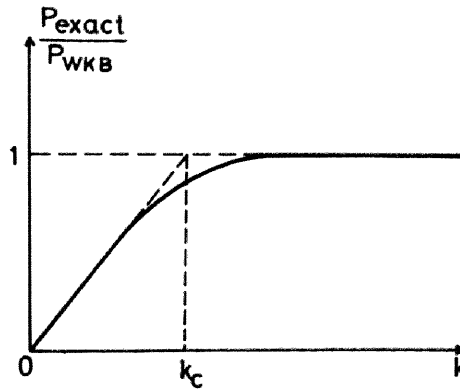


Fig. 1-4. The schematic illustration of the error in the tunneling coefficient by WKB approximation. The exact coefficient vanishes at the band edge. The critical value  $k_c$  is dependent on the model for the potential barrier. ( After R.T. Shuey : Tunneling Phenomena in Solids Ref. 49, p.93. )

# § 1 - 3 Tunneling Spectroscopic Study of Impurity Band ( Purpose of the Research )

The first of the experimental trials to observe the band tail of a heavily doped semiconductor may be the works by Hass<sup>86)</sup> and Pankov.<sup>87)</sup> They studied the optical spectra of a heavily doped germanium and found that the direct (  $\Gamma'_{25} - \Gamma'_2$  ) and indirect (  $\Gamma'_{25} - L_1$  ) band gap are reduced by doping. Recently Tuck<sup>88)</sup> showed that the density of states tail of GaAs decays exponentially into the forbidden band. But to date we haven't known the reliable shape of the density of states of impurity band distinguished from main band.

Tunneling has been one of the useful methods for the study of the band structure of solids. But the fact that the formula for direct tunneling Eq.(1-2) doesn't contain the density of states factor explicitly had made them pessimistic<sup>8)</sup> about the tunneling spectroscopic study of the density of states of semiconductors until Mahan and Conley's investigation in 1966.<sup>28)</sup> They applied WKB approximation and assumed a formula for the current density

$$J = \gamma \int P_{WKB} [ f_R - f_L ] P_R dE \quad (1-7)$$

The problem was, however, more complicated, because it had not been understood precisely how the tunneling transmission probability should behave near the band edge. To make the matter more difficult we cannot apply a simple plane wave for an electron in the impurity band because of the many body aspects.

The applicability of the WKB approximation to the tunneling was first studied by Takeuchi-Funada<sup>89)</sup> and Shuey<sup>90)</sup> independently from a different point of view. They obtained qualitatively same results ; 'the tunneling transmission probability must vanish at the band edge ( or zero of wave vector )'. This fact was studied more rigorously by Duke.<sup>91)</sup> Their analyses are, however, based on a too simplified model to apply them to the investigations of the current-voltage characteristics of real junctions.

The first purpose of our research is to investigate the tunneling probability for a p-n junction exactly. We show in Chap.II that the tunneling probability should have a multiplication factor, which is a function of the density of states of both sides of the junction irrespective

to the shape of the junction potential. On the basis of this result we further study the phenomena of tunneling in an impure semiconductor in the framework of CPA, which is the second purpose. The third is to seek the method of determining the energy spectrum of the impurity band by applying the theory. In Chap.III the current formula is given with the aid of one-electron wave function for an impure-semiconductor and the method to determine the density of states is shown. The formulation includes some assumptions and to overcome the faults partially the theory is further developed in Chap.IV in the frame-work of Hamiltonian formalism with the aid of Green function method. This formula is found to give convincing informations of the energy spectra of the impurity band through the electron self-energy ( self-energy effect ).

The fourth purpose of the research is to study the energy spectra of a heavily doped semiconductor by applying the theories developed above. In Chap.III and Chap.IV the direct current component of a germanium tunnel diode is examined, and the density of states of the impurity band is presented. The results show that the impurity band decays continuously into the forbidden band and that there should be an energy gap between the impurity band and the main band for samples of lower concentrations. The fifth purpose is to study the localized nature of electrons in the metallic concentration region. In Chap.V the anomalous zero bias conductance due to localized magnetic moment is observed, suggesting that impurity band should have localized moment in the immobile states. The reason why we investigate a p-n junction is to avoid the conflicts and ambiguities caused from surface states<sup>92,93)</sup> and any other interactions associated with the indirect transition.

Throughout the article we will pay efforts to make the theory as simple as possible unless we lose the generality of the problem, since the theory of tunneling and impurity band includes many un-solved problems. Our problem is, therefore, how to seek the principle results by experiments, which will give a certain encouragement to the theoretical fields.

## II. TUNNELING AND DENSITY OF STATES

### § 2 - 1 Basic Formulation of Tunneling

We begin with the Hamiltonian for the system which consists of two electrodes separated by a potential barrier as is illustrated in Fig.2-1, where we set the direction of the current flow to the z-axis and the junction plane in the x-y plane:

$$\begin{aligned} H &= H_0 + H' , \\ H_0 &= H_L + H_R , \\ H' &= H_B . \end{aligned} \quad (2-1)$$

In Eq.(2-1) the total Hamiltonian  $H$  should be equivalent to  $H_L$  or  $H_R$  in the limit  $z \rightarrow -\infty$  or  $z \rightarrow +\infty$ , respectively, and we can define eigen states in those limits as

$$\begin{aligned} H_L |q\rangle &= E_q |q\rangle & z \rightarrow -\infty , \\ H_R |k\rangle &= E_k |k\rangle & z \rightarrow +\infty . \end{aligned} \quad (2-2)$$

Thus another Hamiltonian  $H_B$ , which corresponds to the potential barrier, may be considered as a perturbation. According to the time dependent perturbation theory the transition probability due to  $H'$  is given by<sup>94)</sup>

$$P_{L-R} = \frac{\hbar}{\hbar} |\langle q | H' | k \rangle|^2 . \quad (2-3)$$

The tunneling current from the left hand side electrode to the right can be expressed by using Eq.(2-3) and the occupation probability of states as follows

$$j_{L-R} = 2e \sum_{qk} f_L (1 - f_R) P_{L-R} , \quad (2-4)$$

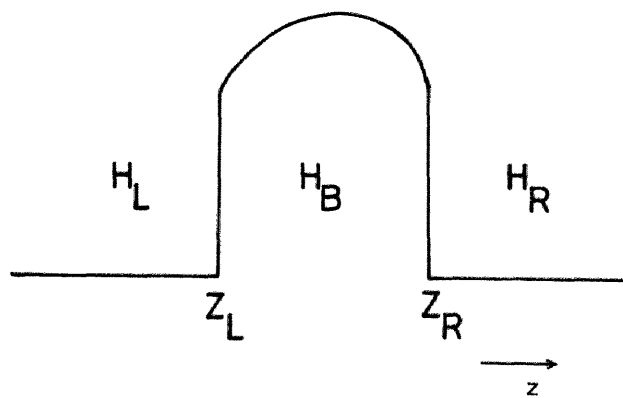


Fig. 2-1. The Hamiltonians for a tunneling junction. The junction potential is assumed to be a function only of  $z$ .

and that from right to left

$$j_{R-L} = 2e \sum_{qk} f_R (1 - f_L) P_{R-L} , \quad (2-5)$$

where the factor 2 comes from the spin degeneracy. By virtue of the symmetry of the matrix element<sup>90)</sup>

$$\langle q | H_B | k \rangle = \langle -k | H_B | -q \rangle , \quad (2-6)$$

we get the expression for the net current

$$\begin{aligned} J &= j_{L-R} - j_{R-L} \\ &= -2e \sum_{qk} [f_R - f_L] P_{L-R} . \end{aligned} \quad (2-7)$$

Because of the translational symmetry in the plane parallel to the junction plane, we get the restriction to the matrix element

$$\langle q | H_B | k \rangle = T_{qk} \delta_{q_{\perp} k_{\perp}} , \quad (2-8)$$

where suffix  $\perp$  for  $q$  and  $k$  means the component parallel to the junction plane. Thus we can write Eq.(2-7) generally with the aid of the energy conservation law of transition<sup>11)</sup> as

$$J = -2e \sum_{qk} [f_R - f_L] P_{L-R} \delta_{q_{\perp} k_{\perp}} \delta(E_L - E_R) , \quad (2-9)$$

which is just the same formula given by Fredkin-Wannier,<sup>9)</sup> and the problem of tunneling is the calculation of the matrix element  $T_{qk}$  between the eigen states of each electrode.

In the course of the actual calculations we often find it more convenient to transform Eq.(2-9) as follows

$$J = -2e \sum_q \langle V_{q_{\parallel}} \rangle P [f_R - f_L] , \quad (2-10)$$

where

$$P = \frac{1}{\pi \hbar} \frac{1}{\langle V_{q_{\parallel}} \rangle \langle V_{k_{\parallel}} \rangle} P_{L-R} \quad (2-11)$$

is called the tunneling probability and the group velocity is given by<sup>12)</sup>

$$\langle v_{q_{\parallel}} \rangle = \frac{1}{\hbar} \frac{\partial E_L}{\partial q_{\parallel}} \quad \text{and} \quad \langle v_{k_{\parallel}} \rangle = \frac{1}{\hbar} \frac{\partial E_R}{\partial k_{\parallel}} \quad . \quad (2-12)$$

Another transformation is also convenient;

$$J = -2e \sum_q \langle v_{k_{\parallel}} \rangle |\mathcal{T}_k|^2 [f_R - f_L] \quad , \quad (2-13)$$

where

$$\mathcal{T}_k = \frac{\sqrt{\pi}}{\hbar \langle v_{k_{\parallel}} \rangle} \langle q | H_B | k \rangle \quad (2-14a)$$

or

$$|\mathcal{T}_k|^2 = \frac{\langle v_{q_{\parallel}} \rangle}{\langle v_{k_{\parallel}} \rangle} \cdot P \quad . \quad (2-14b)$$

$\mathcal{T}_k$  is the transmitted wave amplitude.<sup>12,95)</sup>

If we adopt WKB wave functions for  $|k\rangle$  and  $|q\rangle$ , the tunneling probability  $P_{\text{WKB}}$  is a function only of potential  $V_B$  and energy  $E$ ;

$$P_{\text{WKB}} = \exp \left[ -2 \int_{Z_L}^{Z_R} \kappa \, dz \right] \quad , \quad (2-15)$$

where

$$\kappa = \frac{(2m)^{\frac{1}{2}}}{\hbar} \sqrt{V_B(z) - E} \quad , \quad (2-16)$$

and  $Z_R$  and  $Z_L$  are the classical turning points.<sup>12)</sup>

## § 2 - 2 Tunneling Probability for a p-n junction.

### 2 - 2 - 1. Calculations for Model Potential Barriers

In this subsection we will calculate the tunneling probability for some model junctions and compare them with those of the results by WKB approximation.

#### (a) Rectangular Barrier

The rectangular barrier shown in Fig.(2-2) is the simplest and most idealized junction, which appears in a standard text of quantum mechanics<sup>95)</sup> and studied already by Harrison.<sup>8)</sup> But the results are very instructive to understand the principle of tunneling and we'll show the formulation. The Schrödinger equation for the system is given by

$$\left[ -\frac{\hbar^2}{2m_i} \nabla^2 + V(z) \right] \psi_i = E_i \psi_i, \quad (2-17)$$

where

$$V(z) = \begin{cases} V & (z \leq 0) \\ V_B & (0 \leq z \leq w) \\ 0 & (z \geq w) \end{cases}, \quad (2-18)$$

In order to calculate the transmission amplitude  $\mathcal{T}_k$ , the solution for the Schrödinger equation is given by

$$\begin{aligned} \psi_L &= e^{iq_z z} + \mathcal{R} e^{-iq_z z} & (z \leq 0), \\ \psi_B &= A_1 e^{\kappa_z z} + A_2 e^{-\kappa_z z} & (0 \leq z \leq w), \\ \psi_R &= \mathcal{T}_k e^{ik_z z} & (z \geq w), \end{aligned} \quad (2-19)$$

where we have suppressed the component parallel to the junction plane, i.e.,  $\exp[ik_x x + ik_y y]$ , etc. for the sake of simplicity. (For the time being we will consider only the z-component).  $q_z$ ,  $\kappa_z$  and  $k_z$  are given by the z-component of the energy:



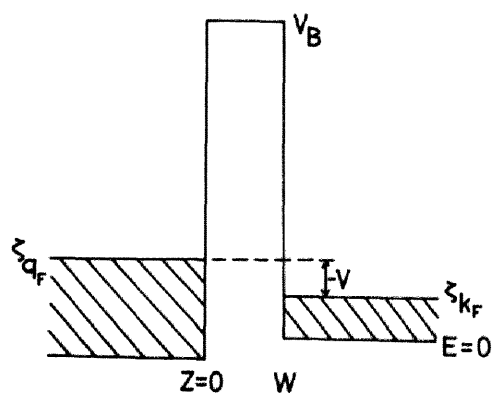


Fig. 2-2. Schematic energy diagram of a rectangular barrier. The energy of the system is measured with respect to the bottom of the conduction band of right hand side electrode.

$$E_{Lz} = \frac{\hbar^2 q_z^2}{2m_L}, \quad E_{Rz} = \frac{\hbar^2 k_z^2}{2m_R} \quad \text{and} \quad V_B - E_{Rz} = \frac{\hbar^2 \kappa_z^2}{2m_B}. \quad (2-20)$$

By using the continuity conditions at  $z = 0$  and  $z = w$ ,

$$\begin{aligned} \psi_i &= \psi_j, \\ \frac{1}{m_i} \nabla_z \psi_i &= \frac{1}{m_j} \nabla_z \psi_j, \end{aligned} \quad (2-21)$$

we get the transmission amplitude of the form

$$T_k = \frac{i4k_z \kappa_z}{m_R m_B} e^{-\kappa_z w} \left( \frac{\kappa_z}{m_B} - i \frac{q_z}{m_L} \right)^{-1} \left( \frac{\kappa_z}{m_B} - i \frac{k_z}{m_R} \right)^{-1}. \quad (2-22)$$

We obtain the tunneling probability

$$P_{\text{rect}} = \frac{16 \nu_L \nu_B^2 \nu_R}{(\nu_L^2 + \nu_B^2)(\nu_R^2 + \nu_B^2)} e^{-2\kappa_z w}, \quad (2-23)$$

where  $\nu_i$  is the group velocity in  $i$ -th region. In the case of a semiconductor junction we get the inequality

$$\nu_L, \nu_R \ll \nu_B, \quad (2-24)$$

and equation (2-23) is approximated by

$$P_{\text{rect}} \approx \frac{16 \nu_L \nu_R}{\nu_B^2} e^{-2\kappa_z w}. \quad (2-25)$$

The tunneling probability by the WKB approximation is given by

$$P_{\text{rect}}^{\text{WKB}} = \exp[-2\kappa_z w]. \quad (2-26)$$

By comparing Eqs.(2-25) and (2-26) we see that the exact transmission probability contained the multiplication factor  $\nu_R \nu_L$ , which is the factor of density of states for parabolic energy band of both electrodes.<sup>96)</sup>

Equation (2-25) is written in an explicit formula for three dimension by

$$P_{\text{rect}} = \frac{16 \nu_L \nu_R}{\nu_B^2} \exp[ - 2 \kappa_0 w ] \exp[ - E_L/E_0 ] \quad , \quad (2-27)$$

$$1/E_0 = (2m_B)^{\frac{1}{2}} / \hbar (V_B - E)^{\frac{1}{2}} \quad . \quad (2-28)$$

#### (b) Uniform Field Barrier

The p-n junction is often approximated by the uniform field model<sup>6,10)</sup> shown in Fig.(2-3), of which potential energy is given by

$$\begin{aligned} V(z) &= V_B - V & (z \leq 0) , \\ &= V_B - V - Fz & (0 \leq z \leq w) , \\ &= 0 & (z \geq w) , \end{aligned} \quad (2-29)$$

where  $F$  is the electric field strength multiplied by the electronic charge  $e$ . Using the same procedure as Eqs.(2-17) - (2-21), the transmission amplitude in the right hand side electrode is given by

$$\mathcal{T}_k = \frac{i \frac{2k_z a}{m_R m_B \pi}}{\left\{ \frac{a}{m_B} B'_i(z_2) - i \frac{k_z}{m_R} B_i(z_2) \right\} \left\{ \frac{a}{m_B} A'_i(z_1) - i \frac{q_z}{m_L} A_i(z_1) \right\}} \quad , \quad (2-30)$$

where  $A_i(z)$ ,  $B_i(z)$  are the Airy's function and  $A'_i(z)$ ,  $B'_i(z)$  their derivatives.<sup>97)</sup> By using the asymptotic formulae for  $A_i(z)$  and  $B_i(z)$ , the tunneling probability is derived as follows,

$$P = \frac{(4q_z k_z m_B^2) / (\pi m_L m_R a^2) \cdot \sqrt{Z_2} \exp[ - 2\zeta ]}{\left\{ Z_2 + \frac{m_B^2 q_z^2}{m_L^2 a^2} \right\} \left\{ \frac{5^{\frac{2}{3}}}{\Gamma(1/3)^2} + \frac{m_B^2 k_z^2}{m_R^2 a^2} \frac{4^{\frac{4}{3}}}{\Gamma(2/3)^2} \right\}} \quad . \quad (2-31)$$

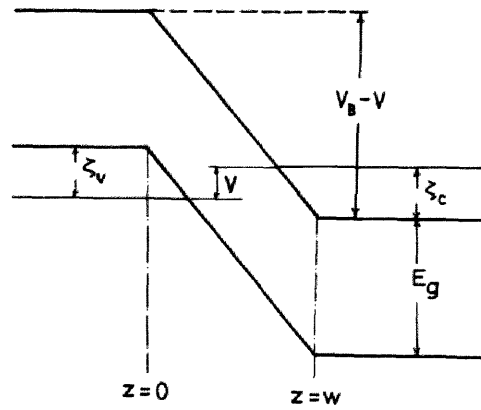


Fig. 2-3. Uniform field model for a p-n junction.

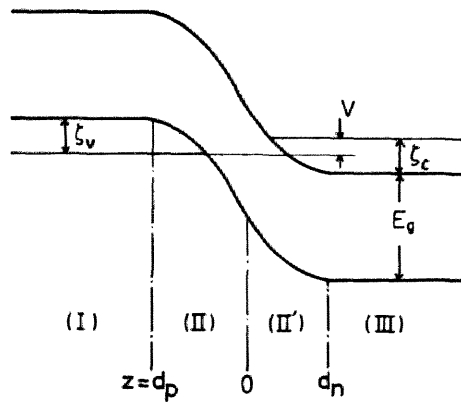


Fig. 2-4. Schematic energy diagram of a parabolic potential barrier. The barrier width  $w = d_n - d_p$  is determined by the Poisson equation with charge density  $eN_L$  ( $d_p \leq z \leq 0$ ) and  $-eN_R$  ( $0 \leq z \leq d_n$ ).

In Eqs.(2-30) and (2-31) several quantities were defined by

$$Z_1 = - \frac{2m_B E_z}{\hbar^2 a^2} , \quad Z_2 = a \left( w - \frac{E_z}{F} \right) , \quad a^3 = \frac{2m_B}{\hbar^2} F \quad \text{and}$$

$$\zeta = \frac{2}{3} \left( \frac{2m_B E_z}{a^2 \hbar^2} \right)^{\frac{3}{2}} . \quad (2-32)$$

In the energy range to be interested or for the energy range corresponding to the band edge, the denominator of Eq.(2-31) varies slowly with respect to energy. Practically it is considered to be constant. The tunneling probability by WKB approximation is given by

$$P_{WKB} = \exp[ - 2\zeta ] . \quad (2-33)$$

Therefore equation (2-31) is proved to have multiplication factors  $(q_z k_z)$ , corresponding to the density of states of both sides.

#### (c) Parabolic Potential Barrier

Parabolic potential barrier is the best model for an abrupt p-n junction.<sup>98)</sup> The potential energy is expressed as follows,

$$\begin{aligned} V(z) &= V_B - V , & ( z \leq d_p ) \\ &= V_B - V - \frac{2\pi N_L e^2}{\epsilon} (z - d_p)^2 , & ( d_p \leq z \leq 0 ) \\ &= \frac{2\pi N_R e^2}{\epsilon} (z - d_n)^2 , & ( 0 \leq z \leq d_n ) \\ &= 0 , & ( z \geq d_n ) \end{aligned} \quad (2-34)$$

where  $V_B$  is the built-in potential,  $N_L$  and  $N_R$  are respectively acceptor and donor concentration and  $\epsilon$  the dielectric constant. The calculation is somewhat lengthy, and the result is given as a function of the parabolic cylinder functions.<sup>99)</sup> By using the asymptotic formula of the functions, after some manipulations, we get the tunneling probability of the

form

$$\begin{aligned}
 P &= \frac{m_L k_z}{m_R q_z} |\mathcal{T}_k|^2 \\
 &= \frac{16 k_z q_z}{\hbar^2 m_R m_L} \exp[ - (y_n^2 + y_p^2)/2 ] \left( \frac{y_p^2}{2} \right)^{\left( \frac{q_z}{r_p} \right)^2} + \frac{1}{2} \left( \frac{y_n^2}{2} \right)^{\left( \frac{k_z}{r_n} \right)^2} + \frac{1}{2} \\
 &\quad \times \left\{ \frac{r_n}{m_R} y_n + \frac{r_p}{m_L} y_p \right\}^{-1} \\
 &\quad \times \left\{ \Gamma^{-2} \left( \frac{1}{4} - \frac{1}{2} \left( \frac{q_z}{r_p} \right)^2 \right) + \frac{1}{2} \left( \frac{q_z}{r_p} \right)^2 \cdot \Gamma^{-2} \left( \frac{3}{4} - \frac{1}{2} \left( \frac{q_z}{r_p} \right)^2 \right) \right\}^{-1} \\
 &\quad \times \left\{ \Gamma^{-2} \left( \frac{1}{4} - \frac{1}{2} \left( \frac{k_z}{r_n} \right)^2 \right) + \frac{1}{2} \left( \frac{k_z}{r_n} \right)^2 \cdot \Gamma^{-2} \left( \frac{3}{4} - \frac{1}{2} \left( \frac{k_z}{r_n} \right)^2 \right) \right\}^{-1}, \quad (2-35)
 \end{aligned}$$

where

$$r_p^4 = \frac{16 \pi m_L N_L e^2}{\hbar^2 \epsilon}, \quad r_n^4 = \frac{16 \pi m_R N_R e^2}{\hbar^2 \epsilon}$$

and

$$y_p^2 = \frac{N_R}{N_L + N_R} \frac{8m_L(V_B - V)}{\hbar^2 r_p^2}, \quad y_n^2 = \frac{N_L}{N_L + N_R} \frac{8m_R(V_B - V)}{\hbar^2 r_n^2}. \quad (2-36)$$

The last two factors in Eq.(2-35) are nearly constant in the low energy region. Hence equation (2-35) can be approximated by

$$P = C_1 q_z k_z \exp[ - \frac{y_p^2 + y_n^2}{2} ] \left( \frac{1}{2} y_p^2 \right)^{\frac{q_z^2}{r_p^2}} \left( \frac{1}{2} y_n^2 \right)^{\frac{k_z^2}{r_n^2}}, \quad (2-37)$$

where  $C_1$  is a constant. In order to simplify the problem let's consider the case of a symmetric junction, i.e., a junction with  $m_L = m_R$  and  $N_L = N_R$ .

This assumption will give no essential error to the conclusion. By virtue of the conservation law of energy and transverse momentum,

$$E_{Rz} + E_{\perp} = \zeta_c + \zeta_v - V - (E_{Lz} + E_{\perp}) , \quad (2-38)$$

equation (2-37) is written by

$$P = C_2 \exp[ -\lambda ] \sqrt{E_{Rz}(\zeta_c + \zeta_v - V - E_{Lz})} \exp[ -\frac{E_{\perp}}{E_0} ] , \quad (2-39)$$

where  $C_2$  is another constant,  $\zeta_c$  and  $\zeta_v$  are the Fermi energy of right and left hand side electrode, respectively. The exponent in Eq.(2-39) is given by

$$\lambda = \frac{V_B - V}{E_{oo}} - \frac{\zeta_c + \zeta_v - V}{2E_{oo}} \ln\left(\frac{V_B - V}{2E_{oo}}\right) , \quad (2-40)$$

where

$$\frac{1}{E_0} = \frac{1}{E_{oo}} \ln\left(\frac{V_B - V}{2E_{oo}}\right) , \quad (2-41)$$

and

$$E_{oo} = \frac{1}{2} \hbar \left( \frac{N_R}{m_R \epsilon} \right)^{\frac{1}{2}} . \quad (2-42)$$

The value of  $\lambda$  varies slowly with respect to the applied bias energy  $V$  and gives similar dependence to the WKB exponent, and the exact tunneling probability is proved to have the multiplication factor  $(q_z k_z)$  corresponding to the density of states of both electrodes.

## 2 - 2 - 2. Arbitrary Potential Barrier

Summarizing the results in Sec.2-2-1, we may generally write the tunneling probability between parabolic energy bands as

$$P = \frac{q_z k_z}{m_L m_R} \exp[ -\lambda ] B(q_z, k_z) \delta_{q_{\perp} k_{\perp}} , \quad (2-43)$$

for an arbitrary potential barrier, and the functional forms of  $\lambda$  and  $B(q_z, k_z)$  should be determined by the shape of the barrier. Actually it is an easy task to prove Eq.(2-43) quite generally. To do this let's go back to Fig.(2-1). The Schrödinger equations are given by the following forms,

$$\begin{aligned}
 - \frac{\hbar^2}{2m_L} \nabla^2 \psi_L &= E_L \psi_L, & (z \leq z_L) \\
 [- \frac{\hbar^2}{2m_B} \nabla^2 + V(z)] \psi_B &= E_B \psi_B, & (z_L \leq z \leq z_R) \\
 - \frac{\hbar^2}{2m_R} \nabla^2 \psi_R &= E_R \psi_R, & (z \geq z_R)
 \end{aligned} \tag{2-44}$$

where  $E_L$ ,  $E_B$  and  $E_R$  should be chosen so as to satisfy the energy conservation law. The solution of Eq.(2-44) is written for each region as

$$\begin{aligned}
 \psi_L &= e^{iq_z z} + R_q e^{-iq_z z}, \\
 \psi_B &= B_1 \phi_1(z) + B_2 \phi_2(z), \\
 \psi_R &= T_k e^{ik_z z},
 \end{aligned} \tag{2-45}$$

in which we have suppressed the component parallel to the junction plane, i.e.,  $\exp[ik_x x + ik_y y]$ , etc. for the sake of simplicity.  $B_1$  and  $B_2$  are the parameters determined by the continuity conditions Eq.(2-21). The two solutions  $\phi_1(z)$  and  $\phi_2(z)$  are assumed to be normalized in the sense

$$W\{\phi_1, \phi_2\} = \begin{vmatrix} \phi_1 & \phi_2 \\ \phi_1' & \phi_2' \end{vmatrix} = 1, \tag{2-46}$$

which is Wronskian determinant.<sup>100)</sup> By making use of Eq.(2-21) we get the expression for the tunneling probability of the form

$$P = \frac{4}{m_B^2} \frac{q_z k_z}{m_L m_R} |\Delta|^{-2}, \tag{2-47}$$



where

$$\begin{aligned}
 \Delta &= \left\{ \frac{\phi_1'(z_L)}{m_B} + \frac{iq_z}{m_L} \phi_1(z_L) \right\} \left\{ \frac{\phi_2'(z_R)}{m_B} - \frac{ik_z}{m_R} \phi_2(z_R) \right\} \\
 &\quad - \left\{ \frac{\phi_1'(z_R)}{m_B} - \frac{ik_z}{m_R} \phi_1(z_R) \right\} \left\{ \frac{\phi_2'(z_L)}{m_B} + \frac{iq_z}{m_L} \phi_2(z_L) \right\} \\
 &= \phi_1(z_L) \phi_2(z_R) \left\{ \frac{1}{m_B} \frac{\phi_1'(z_L)}{\phi_1(z_L)} + \frac{iq_z}{m_L} \right\} \left\{ \frac{1}{m_B} \frac{\phi_2'(z_R)}{\phi_2(z_R)} - \frac{ik_z}{m_R} \right\} \\
 &\quad - \phi_1(z_R) \phi_2(z_L) \left\{ \frac{1}{m_B} \frac{\phi_1'(z_R)}{\phi_1(z_R)} - \frac{ik_z}{m_R} \right\} \left\{ \frac{1}{m_B} \frac{\phi_2'(z_L)}{\phi_2(z_L)} + \frac{iq_z}{m_L} \right\} . \quad (2-48)
 \end{aligned}$$

By the way the functions  $\phi_\alpha(z)$  are the solutions of the wave equation

$$\frac{d^2 \psi}{dz^2} + \frac{2m}{\hbar^2} (E - V) \psi = 0 . \quad (2-49)$$

In the potential barrier we see

$$E - V < 0 , \quad (2-50)$$

that is,  $d^2 \psi / dz^2$  has the same sign as  $\psi$ , so that  $\phi_1$  and  $\phi_2$  are convex toward the  $z$ -axis. Because the solutions should be given as a certain function including decay factor, we can choose for the solution  $\phi_1$  a monotonously decreasing function of the form

$$\phi_1 = \frac{1}{a_0 + a_1 z + a_2 z^2 + a_3 z^3 + \dots} . \quad (2-51)$$

Then  $\phi_2$  is given by

$$\phi_2 = \phi_1 \int \frac{1}{\phi_1^2} dz , \quad (2-52)$$

which is another formula of Eq. (2-46).<sup>100)</sup> By combining Eqs. (2-51) and (2-52) we see that  $\phi_2$  exhibits a monotonously increasing function of the form

$$\phi_2 = b_0 + b_1 z + b_2 z^2 + b_3 z^3 + \dots . \quad (2-53)$$

Though inequality (2-50) does not hold at  $z = z_L$  and  $z = z_R$ , if the energy are small the values of  $\phi_\alpha'$ 's at these points can be approximated by the values of  $\phi_\alpha(z_0)$ , where  $z_0$  is the classical turning points. Consequently we can find an inequality,

$$|\phi_1(z_L)\phi_2(z_R)| \gg |\phi_1(z_R)\phi_2(z_L)|, \quad (2-54)$$

and equation (2-48) can be approximated by

$$\Delta = \phi_1(z_L)\phi_2(z_R) \left\{ \frac{\phi_1'(z_L)}{m_B \phi_1(z_L)} + \frac{iq_z}{m_L} \right\} \left\{ \frac{\phi_2'(z_R)}{m_B \phi_2(z_R)} - \frac{ik_z}{m_R} \right\}. \quad (2-55)$$

Now by putting

$$\lambda = 2 \ln[ \phi_1(z_L)\phi_2(z_R) ], \quad (2-56)$$

we can write Eq.(2-47) as

$$P = \frac{\frac{4}{m_B^2} \cdot \frac{q_z k_z}{m_L m_R} \cdot \exp[ -\lambda ]}{\left| \frac{\phi_1'(z_L)}{m_B \phi_1(z_L)} + \frac{iq_z}{m_L} \right|^2 \cdot \left| \frac{\phi_2'(z_R)}{m_B \phi_2(z_R)} - \frac{ik_z}{m_R} \right|^2}, \quad (2-57)$$

which is just the formula wanted.

As the solutions  $\phi_1(z)$  and  $\phi_2(z)$  are determined by the potential barrier  $V(z)$  in Eq.(2-44), so if  $V(z)$  is large small variation of the energy  $E_B$  will give a negligible effect to the functional forms of the solutions, resulting in the energy insensitive function of  $\lambda$ . The denominator of Eq.(2-57), or

$$B(q_z, k_z) = \frac{4}{m_B^2} \cdot \left| \frac{\phi_1'(z_L)}{m_B \phi_1(z_L)} + \frac{iq_z}{m_L} \right|^{-2} \cdot \left| \frac{\phi_2'(z_R)}{m_B \phi_2(z_R)} - \frac{ik_z}{m_R} \right|^{-2}, \quad (2-58)$$

is also a slowly varying function with respect to energy, and we get

$$B(q_z, k_z) = B(q_z^2, k_z^2). \quad (2-59)$$

Remind that the denominator of Eqs.(2-31) and (2-35) are also written by the form of Eq.(2-59), which enables us to expand them with respect to  $q_z^2$  and  $k_z^2$ . Therefore we get a similar formula to Eq.(2-23) for the lowest

approximation where  $\psi_B$  should be replaced by an appropriate value.

## § 2 - 3 Current Formula and Density of States

By the investigations in the preceding section we have found the tunneling probability for a p-n junction can be written by

$$P = C \exp[-\lambda] \frac{q_z k_z}{m_L m_R} \exp\left[-\frac{E_{\perp}}{E_0}\right], \quad (2-60)$$

where

$$E_{\perp} = \frac{\hbar^2}{2m_R} (k_x^2 + k_y^2), \quad (2-61)$$

and  $E_0$  and  $\lambda$  are determined by the junction potential. The tunneling current is given by

$$J = -q \exp[-\lambda] \int dE [f_R - f_L] N(E, V), \quad (2-62)$$

where  $N(E, V)$  is the tunneling density factor defined by

$$N(E, V) = \frac{E^{\frac{3}{2}}}{E_0} \int_0^{t_{\max}} \frac{1}{\sqrt{(1-t)\{\zeta_c + \zeta_v - V - E(1+t)\}}} \exp\left[-\frac{E}{E_0} t\right] dt. \quad (2-63)$$

$t_{\max}$  is given by

$$t_{\max} = \text{Min} \left\{ 1, \frac{\zeta_c + \zeta_v - V - E}{E} \geq 0 \right\}, \quad (2-64)$$

In Eq.(2-63) the energy  $E$  should be measured from the bottom of the energy band in the right hand side electrode.

To illustrate the behaviours of the density of states factor, we will consider some limiting cases;

(a) Higher energy region  $(E/E_0)t_{\max} \gg 1$ .

Equation (2-63) is approximated by

$$N(E, V) \sim \frac{1}{E^{\frac{1}{2}}} (\zeta_c + \zeta_v - V - E)^{\frac{1}{2}}. \quad (2-65)$$

The first and the second factor in Eq.(2-65) corresponds to the parabolic density of states for conduction and valence band, respectively. If  $\epsilon_c$  and  $\epsilon_v$  are large the latter factor can be approximated by a constant, and equation (2-65) is reduced to

$$N(E, V) \sim (\epsilon_c + \epsilon_v - V)^{\frac{1}{2}} E^{\frac{1}{2}} . \quad (2-66)$$

(b) Lower energy region  $(E/E_0)t_{\max} \ll 1$ .

Assuming  $\epsilon_c$  and  $\epsilon_v$  are large enough, we get approximately

$$N(E, V) \sim \frac{2}{3} \frac{\epsilon_c + \epsilon_v - V}{E_0} \cdot E^{\frac{3}{2}} . \quad (2-67)$$

Thus the function is insensitive to the density of states for valence band,<sup>101)</sup> but its dependence on energy is  $3/2$  power law. Duke obtained a similar result for a sharp junction model.<sup>91)</sup>

(c) Intermediate region

The function will be proportional to  $E^n$ , where the value of  $n$  varies with respect to energy. By calculating numerically we found that  $n$  can be approximated by 1.0 in a wide energy region, as will be shown in Fig.(3-1).

Figure (2-5) shows the function of  $N(E, V)$  schematically. As the tunneling current for the WKB approximation is given by

$$\begin{aligned} J &= -2e P_{\text{WKB}} \int dE [f_R - f_L] \int_0^E dE_{\perp} \\ &= -2e P_{\text{WKB}} \int dE [f_R - f_L] E , \end{aligned} \quad (2-68)$$

the corresponding density factor is proportional to  $E$ , which is shown in the figure.

Finally let's consider how to measure  $N(E, V)$  experimentally.<sup>102,103)</sup> If the temperature is assumed absolute zero, the Fermi-Dirac distribution functions  $f_R$  and  $f_L$  can be described by step functions, and the current formula is written by

$$J = \gamma \exp[-\lambda] \int_{\epsilon_c - V}^{\epsilon_c} dE N(E, V) . \quad (2-69)$$

The differential conductance is

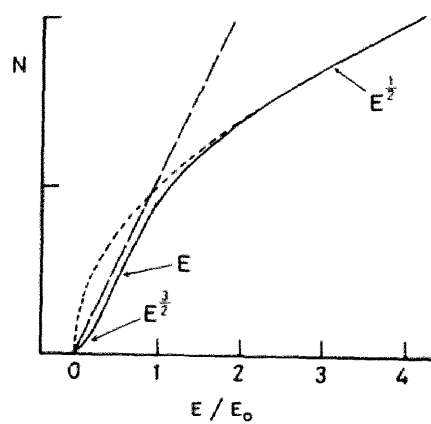


Fig. 2-5. Schematic diagram of the tunneling density factor. In the lower energy region it deviates from parabolicity ( dotted line ). The broken line is that for the WKB formula.

$$\begin{aligned} \frac{dJ}{dV} = & - \frac{d\lambda}{dV} J + \gamma \exp[-\lambda] \int_{\zeta_c^{-V}}^{\zeta_c} dE \frac{\partial N(E, V)}{\partial V} + \frac{\partial \gamma}{\partial V} \frac{1}{\gamma} J \\ & + \gamma \exp[-\lambda] N(E = \zeta_c^{-V}, V) \end{aligned} \quad (2-70)$$

Because the junction potential  $V_B(z)$  is very large, the second and third terms in Eq.(2-70) are very small compared to the remaining terms. We get an approximate formula to determine  $N(E, V)$  :

$$N(E = \zeta_c^{-V}, V) = \gamma^{-1} \exp[\lambda] \left[ \frac{dJ}{dV} + \frac{d\lambda}{dV} J \right] \quad (2-71)$$

In the case of tunneling into (from) states near the band edge, the second term in the bracket of right hand side of Eq.(2-71) is often very small and we can neglect it. Thus we know that tunneling is a powerful method to determine the density of states in semiconductors.

### III. TUNNELING INTO IMPURITY BAND ( I )

#### One Electron Approximation

#### § 3 - 1 One Electron Wave Function

The problem of tunneling in solids is how to solve the Schrödinger equation describing the system, and tunneling across a potential barrier can take place between eigen states of each electrode. We will start out the problem of tunneling into impurity band with the construction of one-electron wave function for an impure semiconductor.

The most important feature which determines the properties of the density of states tail in a semiconductor is the randomness of the distribution of impurities,<sup>56,62)</sup> which can be described by the Hamiltonian

$$H = H_0 + H' \quad . \quad (3-1)$$

In the above expression  $H_0$  is the Hamiltonian for an ideally pure semiconductor and given by

$$H_0 = \frac{1}{2m} p^2 \quad , \quad (3-2)$$

basing on an effective-mass approximation, where  $p$  is the canonical momentum and  $m$  the effective mass of electron.  $H'$  is the potential energy due to impurities

$$H' = \sum_{n=1}^{N_i} v(r - R_n) \quad , \quad (3-3)$$

where  $v(r - R_n)$  is the potential due to  $n$ -th impurity at a site  $R_n$  and  $N_i$  the number density of the impurity atoms. In Eq.(3-3) we have omitted the energy due to electron-electron interaction, for as was shown by Wolff<sup>104)</sup>

its main effect is to shift the band edge, which has no significant meaning in tunneling characteristics.

Our problem is to solve a differential equation of the form

$$\{E - H_0\} \psi(r) = H' \psi(r) , \quad (3-4)$$

where  $H_0$  is written as

$$H_0 = -\frac{\hbar^2}{2m} \nabla^2 . \quad (3-5)$$

With the aid of the Green function satisfying

$$\{E - H_0\} G_0(r, r') = \delta(r, r') , \quad (3-6)$$

we may write the solution of Eq.(3-4) as<sup>105)</sup>

$$\psi(r) = \phi(r) + \int G_0(r, r') H'(r') \psi(r') dr' , \quad (3-7)$$

where  $\phi(r)$  is the solution for the differential equation

$$\{E - H_0\} \phi(r) = 0 . \quad (3-8)$$

We'll rewrite above equations in an operator language,<sup>106)</sup> for the sake of convenience of the following formulation. Equation (3-7) is written as

$$\begin{aligned} \psi_k(r) &= \langle r | k \rangle \\ &= \langle r | k \rangle + \langle r | G_0 H' | k \rangle , \end{aligned} \quad (3-9)$$

where

$$G_0 = \frac{1}{E - H_0 + i0} , \quad (3-10)$$

and  $|k\rangle$  and  $|k\rangle$  are the state vector of  $H$  and  $H_0$ , respectively;



$$H|k\rangle = E|k\rangle, \quad (3-11)$$

$$H_0|k\rangle = \varepsilon_k|k\rangle. \quad (3-12)$$

By virtue of Eq.(3-12) we get the diagonality of the Green function

$$\begin{aligned} \langle k|G_0|k'\rangle &= G_0(k) \delta_{kk'}, \\ &= \frac{1}{E - \varepsilon_k + i\delta}. \end{aligned} \quad (3-13)$$

Now the state vector  $|k\rangle$  is given by iteration in terms of Born series<sup>107,108)</sup>

$$|k\rangle = |k\rangle + G_0 H' |k\rangle + G_0 H' G_0 H' |k\rangle + \dots \quad (3-14)$$

By introducing a new Green function defined by

$$\begin{aligned} G &= \frac{1}{E - H} = \frac{1}{E - H_0 - H'} \\ &= \frac{1}{E - H_0} + \frac{1}{E - H_0} H' \frac{1}{E - H} \end{aligned} \quad (3-15)$$

or

$$G = G_0 + G_0 H' G, \quad (3-16)$$

equation (3-14) is written in a more convenient formula

$$|k\rangle = |k\rangle + G H' |k\rangle, \quad (3-17)$$

which is familiar in the theory of scattering.<sup>105)</sup> But here  $H'$  is not due to single scattering center but consists of potential due to many impurities, which distribute over the volume at random. Equation (3-16) is written in an explicit form as

$$G = G_0 + \sum_{m=1}^{N_i} G_0 v(r-R_m) G, \quad (3-18)$$

which expresses one of the features of the many body problem, that is, electrons interact each other by way of the impurity potential as the super-exchange

interaction.<sup>54)</sup> As was already mentioned (Sec. 1-2), in a random system any physical properties are meaningless without averaging procedure. Here we will apply the diagram perturbation method developed by many authors.<sup>43,109)</sup> In order to seek the analytical formula of Eq.(3-17) let's consider the matrix element of  $GH'$  between  $|k\rangle$ ;

$$\begin{aligned}
 (GH')_{kk'} &= (k|GH'|k') \\
 &= G_o(k) \sum_{n_1}^{N_i} v_{kk'}(R_{n_1}) \\
 &\quad + G_o(k) \sum_{k''} \sum_{n_1}^{N_i} v_{kk''}(R_{n_1}) G_o(k'') \sum_{n_2}^{N_i} v_{k''k'}(R_{n_2}) \\
 &\quad + \dots\dots\dots,
 \end{aligned} \tag{3-19}$$

where

$$v_{kk'}(R_n) = (k|v(r-R_n)|k'), \tag{3-20}$$

and use of Eq.(3-13) has been made of. Equation (3-19) is written diagrammatically as

$$GH' = \text{---} \textcircled{\bullet} \text{---} = \text{---} \overset{\times}{\text{---}} \text{---} + \text{---} \overset{\times}{\text{---}} \overset{\times}{\text{---}} \text{---} + \text{---} \overset{\times}{\text{---}} \text{---} + \dots\dots\dots, \tag{3-21}$$

where solid line represents the Green function  $G_o(k)$  and the cross above the interaction line means the random sum over the impurity sites. The averaged Green function  $\langle G \rangle_{av}$  may be written as follows

$$\begin{aligned}
 \langle G \rangle_{av} &= \text{---} \textcircled{\bullet} \text{---} = \text{---} + \text{---} \textcircled{\bullet} \text{---} \\
 &= \text{---} + \text{---} \overset{\times}{\text{---}} \text{---} + \text{---} \overset{\times}{\text{---}} \overset{\times}{\text{---}} \text{---} + \text{---} \overset{\times}{\text{---}} \text{---} + \dots\dots\dots,
 \end{aligned} \tag{3-22}$$

and the self-energy

$$\Sigma = \text{diagram with a circle and a cross} = \text{diagram with a cross} + \text{diagram with a cross and a loop} + \text{diagram with a cross and two loops} + \text{diagram with a cross and three loops} + \dots, \quad (3-23)$$

Thus we get

$$\langle GH' \rangle_{av} = \langle G \rangle_{av} \Sigma, \quad (3-24)$$

and

$$\langle G \rangle_{av} = G_0 + G_0 \Sigma \langle G \rangle_{av}. \quad (3-25a)$$

Equation (3-25a) is called Dyson's equation, a basic equation for the many body problem, and written by an equivalent formula

$$\langle G \rangle_{av}^{-1} = G_0^{-1} - \Sigma. \quad (3-25b)$$

Combining Eqs.(3-17), (3-24) and (3-25b) we find the wave function written by

$$\begin{aligned} \psi_k(r) &= \langle r|k \rangle \\ &= \langle r|k \rangle + \langle r|\langle GH' \rangle_{av}|k \rangle \\ &= \langle r|k \rangle + \sum \langle r|k' \rangle (k'|\langle GH' \rangle_{av}|k) \\ &= \langle r|k \rangle + \sum \langle r|k' \rangle (k'|\langle G \rangle_{av} \Sigma |k) \\ &= \langle r|k \rangle + \sum \langle r|k' \rangle (k'|\frac{1}{G_0^{-1} - \Sigma}|k'') (k''|\Sigma |k), \end{aligned} \quad (3-26)$$

$$(3-27)$$

and our problem is reduced to the calculation of the matrix element of self-energy  $(k|\Sigma|k')$ . Equation (3-27) says that the new state  $\psi_k(r)$  is described by the linear combination of the complete set  $\{\langle r|k \rangle\}$  for a pure material, and the factor  $(k'|\langle GH' \rangle_{av}|k)$  corresponds to the coefficient. This is similar to that given by the plane wave method for band theory of solids<sup>96)</sup> and essentially same results for a single impurity are given by Ning-Sah<sup>110)</sup> and Blaker-Harris.<sup>111)</sup> According to Eq.(3-23)  $\Sigma_{kk'}$  is given by

$$\Sigma_{kk'} = (k|\Sigma|k')$$

$$\begin{aligned}
&= \sum_{n_1}^{N_i} v_{kk'}(R_{n_1}) + \sum_{k''}^{N_i} \sum_{n_1}^{N_i} \sum_{n_2}^{N_i} v_{kk''}(R_{n_1}) G_0(k'') v_{k''k'}(R_{n_2}) \\
&\quad + \dots\dots\dots,
\end{aligned} \tag{3-28}$$

of which calculation is somewhat complicated. If the potential  $v(r - R_n)$  is of short range approximated by a  $\delta$ -well potential

$$v(r - R_n) = U_0 \delta(r - R_n), \tag{3-29}$$

equation (3-28) can be calculated straight forwardly and  $\Sigma_{kk'}$  is proved diagonal and a function only of energy  $E$  as

$$\Sigma_{kk'} = \Sigma(E) \delta_{kk'}, \tag{3-30}$$

where we have replaced the random sum by the random average<sup>66)</sup>

$$\sum_n^{N_i} = N_i \int dR. \tag{3-31}$$

Equation (3-30) is proved generally by Saitoh et al.,<sup>112)</sup> and described implicitly by Yonezawa<sup>68)</sup> and Sawaki et al.<sup>113)</sup> Equation (3-27) is thus reduced to

$$\begin{aligned}
\psi_k(r) &= \langle r|k \rangle + \langle r|k \rangle \frac{\Sigma(E)}{E - \epsilon_k - \Sigma(E)} \\
&= \phi_k(r) F(E, \epsilon_k, N_i, U_0),
\end{aligned} \tag{3-32}$$

where

$$\phi_k(r) = \langle r|k \rangle, \tag{3-33}$$

and

$$F(E, \epsilon_k, N_i, U_0) = 1 + \frac{\Sigma(E)}{E - \epsilon_k - \Sigma(E)}. \tag{3-34}$$

Equation (3-34) corresponds to the so called wave matrix  $W$ ,<sup>105)</sup> and equation (3-32) shows that for a short range potential we can define a quasi-state described by quantum number  $k$  of which energy is  $E$  (not  $\epsilon_k$ ). In other words, the quantum number is an unknown function of energy

$$k = k(E) \quad , \quad (3-35)$$

or equivalently the energy is an unknown function of  $k$  ;

$$E = E(k) \quad , \quad (3-36)$$

and the functional form should be determined according to the configuration of the impurity distribution and its concentration  $N_i$ . This idea is equivalent to the principle of the coherent potential approximation,<sup>63)</sup> i.e., to define an effective Hamiltonian

$$H_e = H_0 + \Sigma \quad , \quad (3-37)$$

so as to satisfy the requirement that the Green function  $G_e$  of  $H_e$  must be equal to  $\langle G \rangle_{av}$ . Consequently the energy of an electron is given by

$$E = \epsilon_k + \Sigma(E) \quad . \quad (3-38)$$

Actually it is easily shown that Eq.(3-32) also gives the same energy. Thus we can define the density of states by<sup>96)</sup>

$$D(E) = \sum_k \delta(E - E_k) = \frac{1}{2\pi^2} k^2 \frac{\partial k}{\partial E} \quad , \quad (3-39)$$

where spherical symmetry of the state vector has been assumed. In Sec.3-4 we'll discuss in detail about the approximations adopted here.

### § 3 - 2 Current Formula and Density of States

Using the wave function Eq.(3-32) we'll get the expression for the tunneling current into ( or from ) an impure semiconductor, which will give a method to investigate the effects of the density of states tail on electron tunneling. For the sake of simplicity of the calculations some approximations are employed: first, the valence band in p-side is parabolic and the wave function obtained in Sec.3-1 is used only for the n-side region in which energy band has spherical symmetry in k-space. This is a good approximation if we are concerned with the band tail of conduction band in n-side and the Fermi energy in p-side is large enough, for as will be shown in what follows the deformation of the parabolicity of the energy band due to impurity potential is significant only in the small energy region near the band edge.<sup>112)</sup> Secondly, the effect of impurity potential in the barrier region is neglected. In an actual junction, however, the potential fluctuation due to impurity in the depletion layer may have some effects on electron tunneling.<sup>115-118)</sup>

The wave function in the four region is given as follows, referring to Fig.2-4

$$\psi_L = e^{iqr} + R e^{-iqr}, \quad (I)$$

$$\psi_1 = (A_{11} U_1 + A_{12} V_1) e^{i\mathbf{p} \cdot \mathbf{r}}, \quad (II) \quad (3-40)$$

$$\psi_2 = (A_{21} U_2 + A_{22} V_2) e^{i\mathbf{p} \cdot \mathbf{r}}, \quad (II')$$

$$\psi_R = \tilde{T}_k \psi_k, \quad (III)$$

where  $\mathbf{p}$  is the vector component parallel to the junction plane. By adopting the continuity condition Eq.(2-21), the transmission amplitude is calculated and given by

$$|\tilde{T}_k|^2 = |F|^{-2} |\mathcal{T}_k|^2, \quad (3-41)$$

where  $F$  and  $\mathcal{T}_k$  is given by Eq.(2-34) and (2-35), respectively. The tunneling probability is written as follows

$$p_{p-n} = \frac{\langle \tilde{v}_n \rangle}{\langle v_p \rangle} \cdot |\tilde{\mathcal{T}}_k|^2 = \frac{\langle v_n \rangle}{\langle v_p \rangle} \cdot |\mathcal{T}_k|^2, \quad (3-42)$$

where again use of the wave function  $\psi_k$  was made in the expression of the group velocity  $\langle \tilde{v}_n \rangle$ , i.e.,

$$\langle \tilde{v}_n \rangle = \int \psi_k^* \frac{\hbar}{im} \nabla_z \psi_k dr = |F|^2 \langle v_n \rangle, \quad (3-43)$$

and

$$\langle v_n \rangle = \frac{1}{\hbar} \frac{\partial \varepsilon_k}{\partial k_z}. \quad (3-44)$$

Substitution of Eq.(2-35) into Eq.(3-42) gives

$$p_{p-n} = C_3 \langle v_p \rangle \langle v_n \rangle \cdot \exp\left[-\frac{V_B - V}{E_{oo}}\right] \exp\left[\frac{E_{nz} + E_{pz}}{2E_{oo}} \ln \frac{V_B - V}{E_{oo}}\right]. \quad (3-45)$$

where  $C_3$  is a constant and similar approximations for Eq.(2-37) have been employed. By the translational symmetry in the plane parallel to the junction plane the transverse wave vector must be conserved. Assuming  $m_L = m_R$ , the conservation law of energy and transverse wave vector is written as

$$E_{pz} + E_{\perp} = \zeta_c + \zeta_v - V - (E_{nz} + E_{\perp}), \quad (3-46)$$

where  $E_{\perp}$  is equal to

$$E_{\perp} = \frac{\hbar^2}{2m_R} (k_x^2 + k_y^2). \quad (3-47)$$

Combining Eqs.(3-45), (3-46) and (2-10) we get the expression for the tunneling current;

$$J = -q \exp[-\lambda] \int dE [f_R - f_L] N(E, V), \quad (3-48)$$

where

$$N(E, V) = \varepsilon_k \frac{\varepsilon_k}{E_o} \int_0^1 dt \sqrt{(1-t)(\zeta_c + \zeta_v - V - E - \varepsilon_k t)} \exp\left[-\frac{\varepsilon_k}{E_o} t\right], \quad (3-49)$$

$$\varepsilon_k = \frac{\hbar^2 k^2}{2m_R}, \quad (3-50)$$

and  $\lambda$  is given by Eq.(2-40). Equation (2-49) is just the same formula for a pure material Eq.(2-39) and doesn't contain the correction function  $F$ , and suggesting that we can know the effect of the impurity potential via the energy dependence of  $\varepsilon_k$ ,

$$\varepsilon_k = \varepsilon_k(E), \quad (3-51)$$

which is equivalent to Eq.(3-35). If we are restricted ourselves to the investigation of the characteristics for the band tail in n-type electrode the inequality holds,<sup>119)</sup>

$$\zeta_v \gg \varepsilon_k, \quad (3-52)$$

and equation (3-49) is approximated by

$$N(E,V) = (\zeta_c + \zeta_v - E - v)^{\frac{1}{2}} \cdot \varepsilon_k^{\frac{1}{2}} \frac{\varepsilon_k}{E_0} \int_0^1 dt (1-t)^{\frac{1}{2}} \cdot \exp\left[-\frac{\varepsilon_k}{E_0} t\right]. \quad (3-53)$$

Figure (3-1) is the dependence of  $N(E,V)$  as a function of  $\varepsilon_k$  in the lower energy region. If we approximate Eq.(3-53) by a linear function

$$N(E,V) = a \cdot \varepsilon_k, \quad (3-54)$$

the density of states near the band edge is given as a function of tunneling density factor as follows

$$\begin{aligned} D(E = \zeta_c - V) &= \frac{1}{2\pi^2} k^2 \frac{\partial k}{\partial E} = \frac{(2m)^{\frac{3}{2}}}{4\pi^2 \hbar^3} \varepsilon_k^{\frac{1}{2}} \frac{\partial \varepsilon_k}{\partial E} \\ &\propto N(\zeta_c - V, V)^{\frac{1}{2}} \frac{\partial N(\zeta_c - V, V)}{\partial (\zeta_c - V)}, \end{aligned} \quad (3-55)$$

where use of Eq.(3-39) and Eq.(3-51) was made. Thus combining Eqs.(2-71) and (3-55), we can investigate the density of states as a function of applied bias energy.



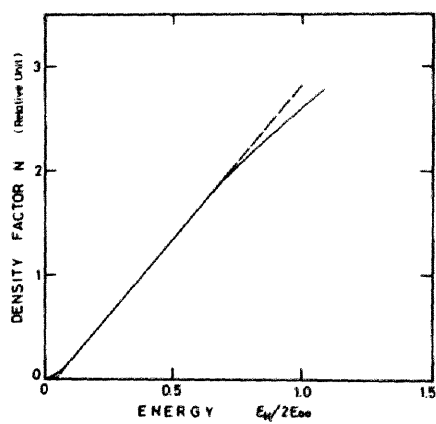


Fig. 3-1. The linear approximation for the tunneling density factor.

### § 3 - 3 Experimental Investigation of Density of States

By making use of the method given in the previous section we'll investigate the density of states of (000) valley of n-type germanium. Germanium is an indirect gap type semiconductor<sup>120)</sup> and the tunneling current under the usual operation is due to the indirect transition between the top of the valence band ( $\Gamma_{25}'$ ) and the bottom of the conduction band (L). But in the reverse current there is a marked increase (Kane Kink) corresponding to the onset of the band-to-band direct transition;<sup>121)</sup> the transition between the top of the valence band and the bottom of the subsidiary conduction band minimum at the zone-center ( $\Gamma_2'$ ). Beyond the Kane Kink the total current  $J$  can be written as a sum of the indirect current component  $I_i$  and the direct current component  $I_d$ .<sup>16)</sup>  $I_i$  is well described by the formula given by Price, Radcliffe<sup>122)</sup> and Kane<sup>6)</sup> (PRK),

$$I_i = \alpha V \exp[-\beta V] \quad , \quad (3-56)$$

in which  $\alpha$  and  $\beta$  should be determined experimentally.<sup>123,124)</sup> By applying Eq.(3-56) we can eliminate the direct current component from experimental data as is shown in Fig.(3-3) schematically.

In the case of the indirect transition, because of the conservation law of momentum, electron cannot transfer without an aid of phonon or any other excitations,<sup>22,125)</sup> and we must take properly into account these effects. In contrast to the complicated nature of the indirect transition, the tunneling current due to direct transition, which is just the current we have ever considered in this work, is much simpler to investigate the effect of impurity band. Another difficulty in tunneling is the zero bias conductance anomaly (ZBA) observed at low temperature even in junctions made of direct gap type semiconductors.<sup>34)</sup> The ZBA is, however, sensitive to temperature and the energy width is less than 50 meV around  $V=0$ . Therefore in the investigations of the direct current in a germanium tunnel diode ( $V < -90$  meV), we can neglect all of these inelastic and indirect tunneling transition.

The material is a germanium single crystal doped with As or Sb atoms. The donor concentrations were 5 and  $15 \times 10^{18} \text{ cm}^{-3}$  for As and 5 and  $13 \times 10^{18} \text{ cm}^{-3}$  for Sb. The tunnel junctions were made by alloying InGa (Ga 0.5%) at about 550°C. The current( $J$ )-voltage( $V$ ) and the incremental resistance  $dV/dJ - V$  were measured at liq.He temperature. To

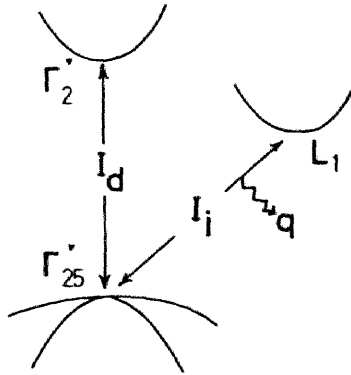


Fig. 3-2. Schematic diagram of tunneling transitions in a germanium tunnel diode. The direct transition takes place between the top of the valence band and the bottom of the conduction band minimum ( $\Gamma'_2$ ). In the case of the indirect transition ( $\Gamma'_{25} \leftrightarrow L_1$ ), the momentum is conserved with the aid of phonons.

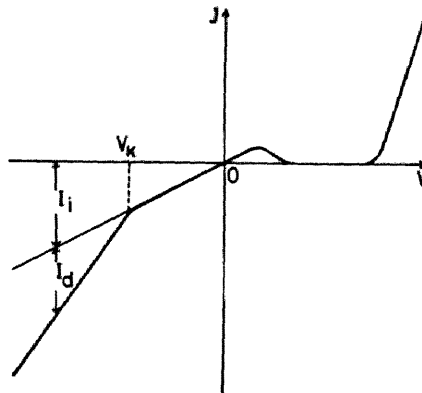


Fig. 3-3. Schematic current-voltage characteristics of a germanium tunnel diode. In the reverse current there is a threshold voltage  $V_k$  corresponding to the onset of direct transition. The diode current is given as a sum of indirect current  $I_i$  and direct current  $I_d$ .

trace the  $dV/dJ - V$  curves the harmonic technique was used;<sup>126)</sup> the superposed alternating signal was 500 Hz and less than 100  $\mu\text{Vp-p}$ .

In Fig.(3-4) typical plots of PRK relation for Sb doped samples are shown. From the linearity in the lower energy region we can determine the parameters  $\alpha$  and  $\beta$  for Eq.(3-56). By subtracting the contribution of the indirect current we get the  $I_d - V$  and  $dI_d/dV - V$  curves as is shown in Fig.(3-5). By making use of Eq.(2-71) the tunneling density factor  $N$  is obtained; the result for a Sb doped sample is shown in Fig.(3-6), where the junction parameter  $E_o$  is estimated to be about 0.016 eV. In the higher energy region they exhibit the parabolic behaviour of the tunneling density factor in good agreement with the theoretical results. The effective mass of electron and hole is  $m_e = 0.041m_o$  and  $m_h = 0.043m_o$ , respectively.<sup>127)</sup> The junction parameter  $E_o$  is estimated to be  $E_o = 0.02$  eV for  $N_d = 5 \times 10^{18} \text{ cm}^{-3}$  and 0.05 eV for  $1.5 \times 10^{19} \text{ cm}^{-3}$  for a bias energy region measured ( $100 < -V < 150$  meV). Thus the linear approximation Eq.(3-54) seems valid for the lower energy region. We applied the approximated formula Eq.(3-55) and the results are shown in Fig.(3-7), where we have reproduced the parabolic behaviour of the density of states in the main band. The deviation from the parabolic relation around the band edge is the incremental evidence of the impurity band ( band tail ). The sharp dip for As doped sample suggests that there should exist an energy gap between the impurity band and the main band for much lower concentrations. The results will be discussed fully in Sec.4-4, but the following features are demonstrated now;

- (a) The results prove the existence of the virtual energy level associated with the (000) subsidiary valley of germanium.<sup>128)</sup>
- (b) The impurity band decays continuously into the forbidden band, and its behaviour depends on the dopant. For As doped sample, the density of states of impurity band is asymmetric around its maximum,<sup>66)</sup> i.e., the exponential tail in the lower energy side but a sharp drop in the higher side. In the case of Sb doped sample, however, there is no evidence of the dip, and the long tail can be described by the relation

$$D(E) \propto \exp[ - |E|^n ] , \quad (3-57)$$

where  $n$  varies smoothly from 0.5 to 2.0 as is shown in Fig.3-8.<sup>71)</sup>

- (c) The results satisfy the Friedel's Sum Rule,<sup>61,105,129)</sup> i.e., the integrated density of states is equal to the integrated density of states of the

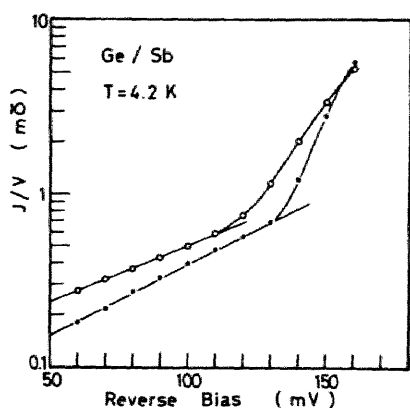


Fig. 3-4. Typical plots of PRK relation for Sb doped samples. From the linearity in the smaller bias region, the values of  $\alpha$  and  $\beta$  are determined. The donor concentration of the sample is  $1.3 \times 10^{19} \text{ cm}^{-3}$  (o) and  $5 \times 10^{18} \text{ cm}^{-3}$  (•).

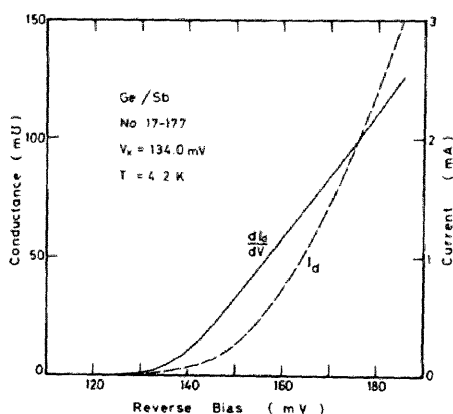


Fig. 3-5. Typical curves for the direct current component for a Sb doped germanium tunnel diode. The donor concentration is  $5 \times 10^{18} \text{ cm}^{-3}$ .

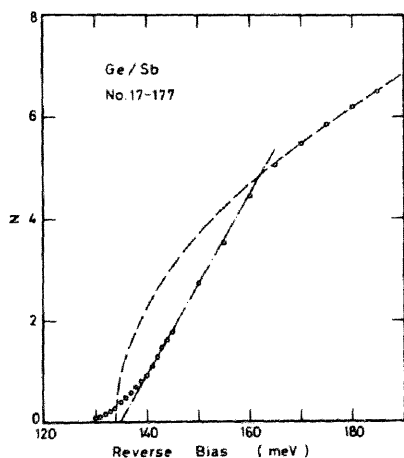


Fig. 3-6. The tunneling density factor for a Sb doped sample. The curve should be compared with Fig. 2-5.

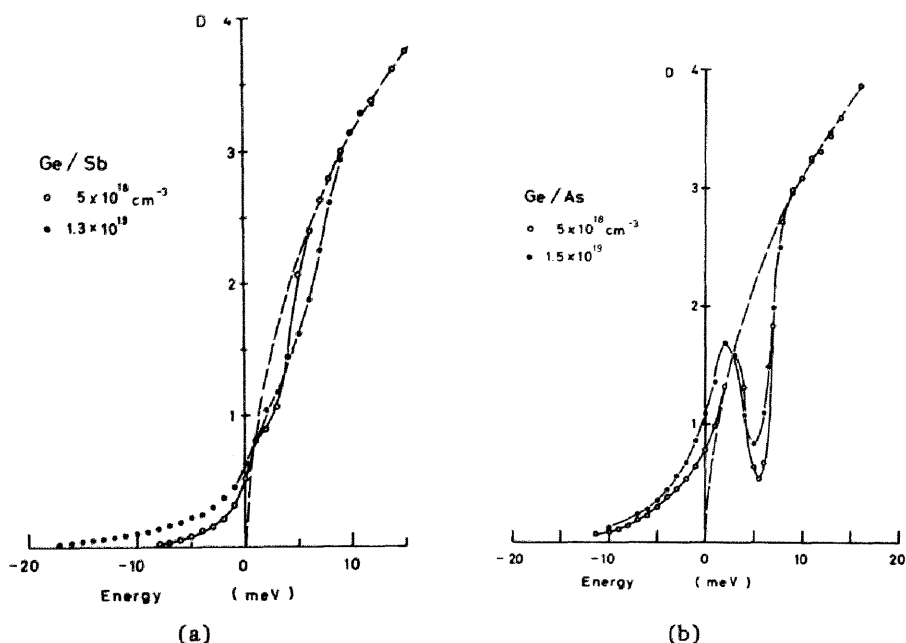


Fig. 3-7. Density of states in the lower energy region. The energy are measured from the parabolic band edge determined by extrapolating the parabolicity in the higher energy region ( broken line ).

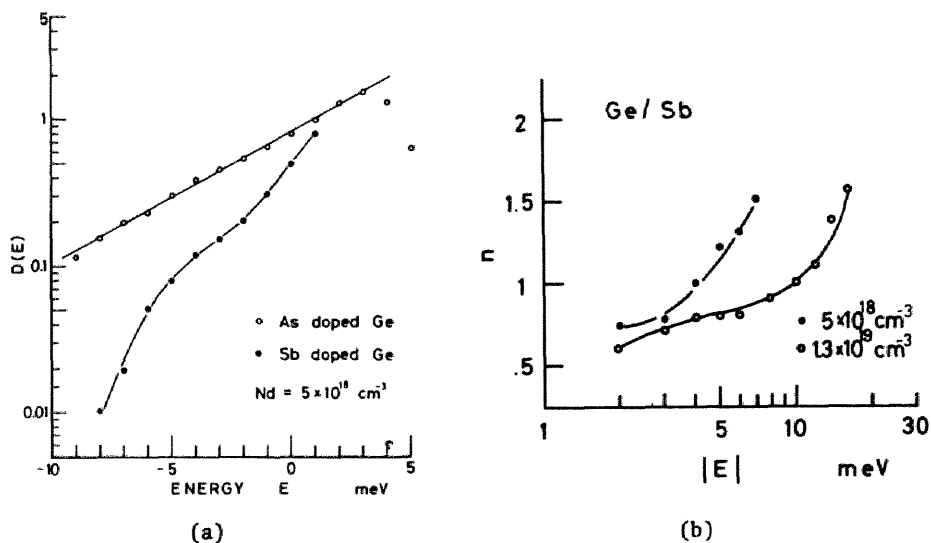


Fig. 3-8. The density of states in the lower energy region of the impurity band. As doped sample exhibits a simple exponential decay. In the case of Sb doped sample it is expressed by  $D(E) \sim \exp[-|E|^n]$ , and  $n$  is a function of energy shown in (b).

parabolic band irrespective to dopant and its concentrations. This fact is thought to prove the validity of the theory, because the donor atoms is expected to distribute substitutionally.

### § 3 - 4 Notes on the Quasi-Particle Approximation

Before concluding this chapter we'll make it clear what approximations we have adopted in Eq.(3-39) and therefore in Eq.(3-55). As was already mentioned, the application of the one-electron wave function given by Eq.(3-32) is equivalent to the simplest form of CPA,

$$E = \varepsilon_k + \Sigma(E) \quad . \quad (3-58)$$

Consequently the wave vector is given as a real quantity

$$k = \frac{(2m)^{\frac{1}{2}}}{\hbar} (E - \Sigma)^{\frac{1}{2}} \quad , \quad (3-59)$$

and now  $k$  loses its original meaning as a quantum number for the bare particle and it should be thought as a quantum number of a quasi-particle. This relation did make it possible to combine Eqs.(3-55) and (3-49). However turning to Eq.(3-27), the electronic state is given as a linear combination of the original (bare particle) representation. If the diagonality of the self-energy does not hold, the one-to-one correspondence between the original representation and the quasi-particle picture becomes meaningless. Actually by writing Eq.(3-27) as

$$\psi_k(r) = \phi_k(r) (1 + a_{kk'} \delta_{kk'}) + \sum_{k' \neq k} \phi_{k'}(r) a_{k'k} \quad , \quad (3-60)$$

where

$$a_{k'k} = \sum_{k''} \langle k' | \frac{1}{G_0^{-1} - \Sigma} | k'' \rangle \langle k'' | \Sigma | k \rangle \quad , \quad (3-61)$$

it is expected that tunneling can take place into all of the bare particle states. Therefore Eq.(3-41) must be corrected properly. Similarly the

concepts of the group velocity Eq-(3-43) is doubtful, which is shown by re-writing Eq.(3-43) as

$$\langle \tilde{v}_n \rangle = |1 + a_{kk'} \delta_{kk'}|^2 \langle v_k \rangle + \sum_{k' \neq k} |a_{k',k}|^2 \langle v_{k'} \rangle \quad (3-62)$$

The non-zero of Eq.(3-61) for  $k' \neq k$  means the transition between the bare particle states, consequently the group velocity defined by Eq.(3-62) is not the constant of motion. To date it hasn't been known how much the contribution of the off-diagonal elements is, and we cannot know the correctness of the procedure to investigate the density of states.

One way to generalize the problem is to treat tunneling in the bare-particle description. As will be shown in the next chapter the density of states and the Green function is connected by the relation

$$D(E) = - \sum_{kk'} \frac{1}{\pi} \text{Im} G(kk'; E) \delta_{kk'} \quad , \quad (3-63)$$

where

$$G(kk'; E) = \langle k | \langle G \rangle_{av} | k' \rangle \quad . \quad (3-64)$$

In this bare particle representation, the self-energy  $\Sigma(E)$  is generally a complex reflecting the finite life of the bare particle state. Thus by putting

$$\Delta = \text{Re } \Sigma(E) \quad , \quad (3-65)$$

and

$$\Gamma = \text{Im } \Sigma(E) \quad , \quad (3-66)$$

equation (3-63) is written as follows

$$D(E) = - \frac{1}{\pi} \sum_k \frac{\Gamma}{(E - \epsilon_k - \Delta)^2 + \Gamma^2} \quad (3-67)$$



$$= \frac{(2m)^{\frac{3}{2}}}{4\pi\hbar^3} \operatorname{Re}(E - \Sigma)^{\frac{1}{2}} \quad (3-68)$$

Equation (3-67) shows that the bare particle state of energy  $\epsilon_k$  is shifted by  $\Delta$  and has a damping  $\Gamma$ , and this nature of description is thought to be partially responsible for the transition of the bare particle states. Actually extending the meaning of the group velocity, equation(3-59) gives the expression for the complex group velocity as<sup>130)</sup>

$$\langle \tilde{v} \rangle = \left( \frac{2m}{\hbar} \right)^{\frac{1}{2}} (E - \Sigma)^{\frac{1}{2}}, \quad (3-69)$$

and the imaginary part of Eq.(3-69) express the decay of the states.

By the way, by combining Eqs.(3-38) and (3-39) we get the state density of the form

$$D(E) = \frac{(2m)^{\frac{3}{2}}}{4\pi\hbar^3} (E - \Sigma)^{\frac{1}{2}} \left( 1 - \frac{\partial \Sigma}{\partial E} \right), \quad (3-70)$$

which is just the same formula given for the quasi-particle approximation, where we have only to replace  $\Sigma$  by  $\Delta$ .<sup>131)</sup> Thus by using the one-electron wave function, we have neglected the damping as well as the off-diagonality.

In the next chapter we will formulate the theory of tunneling in the bare particle representation in order to generalize the treatment, where the imaginary part of the self-energy will be taken into account.

Finally let's take a glance at the localization of the electronic states. If an electron is strongly bound at an atomic site, the electronic state cannot be described by a wave function of the form given by Eq.(3-32), which extends uniformly over the whole crystal. It is one of the main faults of our original formula Eq.(3-7). If the material is lightly doped (which is not the case of our tunneling problem), we should start out from the atomic wave function.<sup>66)</sup> The situation may also be the same in the case of an amorphous material. This is, however, beyond our problem.

#### IV. TUNNELING INTO IMPURITY BAND ( II )

##### Self-Energy Effect

#### § 4 - 1 Formulation of the Problem

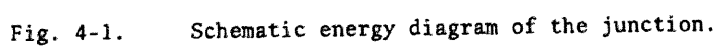
The fault of the current formula Eq.(3-48) was caused by the application of one-electron wave function. To avoid this we'll develop the theory of tunneling in the frame-work of the Hamiltonian formalism established by Bardeen<sup>47)</sup> and developed by Zawadowski<sup>132)</sup> and Appelbaum-Brinkman.<sup>33)</sup>

Our system consists of two electrodes; left hand side electrode labeled as L and right hand side electrode labeled as R, separated by a potential barrier which is thick enough in a sense as will become clear in what follows. In both electrodes electrons travel interacting with impurity potentials, which will be described by the following Hamiltonians;

$$\begin{aligned}
 H &= H_R + H_L + H_B, \\
 H_R &= \sum_k \epsilon_k a_k^\dagger a_k + \sum_k \sum_{k'} V_R(k'-k) a_{k'}^\dagger a_k, \\
 H_L &= \sum_q \epsilon_q b_q^\dagger b_q + \sum_q \sum_{q'} V_L(q'-q) b_{q'}^\dagger b_q + (V_0 + V), \\
 H_B &= \sum_q \sum_k T_{qk} a_k^\dagger b_q + T_{kq} b_q^\dagger a_k,
 \end{aligned} \tag{4-1}$$

where  $a_k^\dagger$ ,  $a_k$ ,  $b_q^\dagger$ , and  $b_q$  is the creation and annihilation operators of electron in the right and left hand side electrode, respectively,  $V_0$  the contact potential and  $V$  is the bias energy applied across the junction.  $V_R(k' - k)$  and  $V_L(q' - q)$  are given by the Fourier transformation of the impurity potential defined by

$$V_R(k' - k) = \sum_{R_n}^{N_R} \int v_R(\mathbf{r} - \mathbf{R}_n) e^{-i(\mathbf{k}' - \mathbf{k}) \cdot \mathbf{r}} d\mathbf{r}, \tag{4-2a}$$



and

$$V_L(q'-q) = \sum_{R_n}^{N_L} \left( v_L(r-R_n) e^{-i(q'-q) \cdot r} dr \right), \quad (4-2b)$$

respectively, where  $v_\alpha(r-R_n)$  is the potential due to individual impurity at a site  $R_n$ , and the summation should be completed over all the impurity sites. The periodic potential of the crystal is compressed into the effective mass as

$$\varepsilon_k = \frac{\hbar^2 k^2}{2m_R}, \quad \varepsilon_q = \frac{\hbar^2 q^2}{2m_L}. \quad (4-3)$$

The Hamiltonian  $H$  should be equivalent to  $H_R$  ( or  $H_L$  ) in the limit  $z \longrightarrow +\infty$  ( or  $z \longrightarrow -\infty$  ) and each electrode is assumed to have a orthonormal set independent of one another ( electrode approximation ). This is described by setting the Hamiltonian, referring to Fig.(4-1), as

$$\begin{aligned} H_O &= H_R & ( z \geq Z_R ) &, \\ &= H_R + H_L & ( Z_L \leq z \leq Z_R ) &, \\ &= H_L & ( z \leq Z_L ) &, \end{aligned} \quad (4-4)$$

which is true if the junction is thick enough to neglect the Hamiltonian of another electrode.<sup>94)</sup> Another Hamiltonian  $H_B$ , which represents the transfer of electrons from one electrode to another, is thus considered perturbation. The transfer matrix  $T_{qk}$  is often called vertex function because of its role in the diagrammatic representation of tunneling.<sup>41)</sup>

In order to obtain the tunneling current across the junction we diagonalize the Hamiltonians  $H_R$  and  $H_L$ ,

$$H_R = \sum_{\mu} E_{\mu} A_{\mu}^{\dagger} A_{\mu}, \quad (4-5a)$$

$$H_L = \sum_{\nu} E_{\nu} B_{\nu}^{\dagger} B_{\nu}, \quad (4-5b)$$

by orthogonal transformations

$$a_k = \sum_{\mu} c_{k\mu} A_{\mu}, \quad (4-6a)$$

$$b_q = \sum_{\nu} c_{q\nu} B_{\nu}^{\dagger}, \quad (4-6b)$$

where  $A_{\mu}^{\dagger}$ ,  $A_{\mu}$ ,  $B_{\nu}^{\dagger}$  and  $B_{\nu}$  are the creation and annihilation operator of  $\mu$ -th eigen state of right hand side electrode and  $\nu$ -th eigen state of left hand side electrode, respectively, and  $E_{\mu}$ ,  $E_{\nu}$  their eigen values. The coefficients  $c_{k\mu}$  and  $c_{q\nu}$  should satisfy the ortho-normality relation:

$$\sum_{\mu} c_{k\mu} c_{k'\mu}^{\dagger} = \delta_{kk'}, \quad (4-7a)$$

$$\sum_{\nu} c_{q\nu} c_{q'\nu}^{\dagger} = \delta_{qq'}. \quad (4-7b)$$

The tunneling transmission current is given, by definition, as

$$J(V, T) = - \int dE j(E) [f_R - f_L], \quad (4-8)$$

where the current density  $j(E)$  is

$$j(E) = \frac{2\pi e}{\hbar} \sum_{\mu\nu} |K_{\nu}|^2 |H_B|_{\mu}^2 \delta(E_{\nu} - E) \delta(E_{\mu} - E), \quad (4-9)$$

where the factor 2 comes from the summation over the electron spin.

In order to rewrite  $j(E)$  in the original representation we introduce Green functions defined by

$$G_R(kk'; E) = \langle 0 | a_k \frac{1}{E - H_R} a_{k'}^{\dagger} | 0 \rangle, \quad (4-10a)$$

$$G_L(qq'; E) = \langle 0 | b_q \frac{1}{E - H_L} b_{q'}^{\dagger} | 0 \rangle, \quad (4-10b)$$

$$G_R^0(kk'; E) = \langle 0 | a_k \frac{1}{E - H_R^0} a_{k'}^{\dagger} | 0 \rangle \quad (4-11a)$$

and

$$G_L^0(qq'; E) = \langle 0 | b_q \frac{1}{E - H_L^0} b_{q'}^{\dagger} | 0 \rangle, \quad (4-11b)$$

where  $|0\rangle$  is the vacuum state and  $H_{\alpha}^0$  is the Hamiltonian for an ideally pure crystal. Substituting Eq.(4-6) into (4-10) and (4-11) we get

$$G_R(kk'; E) = \sum_{\mu} c_{k\mu} c_{k'\mu}^{\dagger} \frac{1}{E - E_{\mu} + i\delta} , \quad (4-12a)$$

$$G_L(qq'; E) = \sum_{\nu} c_{q\nu} c_{q'\nu}^{\dagger} \frac{1}{E - E_{\nu} + i\delta} , \quad (4-12b)$$

$$G_R^0(kk'; E) = \frac{1}{E - \varepsilon_k + i\delta} \delta_{kk'} , \quad (4-13a)$$

and

$$G_L^0(qq'; E) = \frac{1}{E - \varepsilon_q + i\delta} \delta_{qq'} . \quad (4-13b)$$

The Green functions defined by Eqs.(4-10) and (4-11) are equivalent to  $G$  and  $G_0$  introduced by Eqs.(3-15) and (3-16), connected by the following relation,

$$G_{\alpha}(kk'; E) = (k | G_{\alpha} | k') , \quad (4-14)$$

and

$$|k\rangle = a_k^{\dagger} |0\rangle . \quad (4-15)$$

The imaginary part of each Green function is given by

$$\text{Im}G_R(kk'; E) = -\pi \sum_{\mu} c_{k\mu} c_{k'\mu}^{\dagger} \delta(E - E_{\mu}) , \quad (4-16a)$$

and

$$\text{Im}G_L(qq'; E) = -\pi \sum_{\nu} c_{q\nu} c_{q'\nu}^{\dagger} \delta(E - E_{\nu}) , \quad (4-16b)$$

where use of the following relation has been made,

$$\frac{1}{x + i\delta} = P \frac{1}{x} - i\pi\delta(x) . \quad (4-17)$$

The level density of each electrode is given by

$$D_R(E) = \sum_{\mu} \delta(E_{\mu} - E) = -\frac{1}{\pi} \sum_{kk'} \text{Im}G_R(kk'; E) \delta_{kk'} , \quad (4-18a)$$

$$D_L(E) = \sum_{\nu} \delta(E_{\nu} - E) = -\frac{1}{\pi} \sum_{qq'} \text{Im} G_L(qq'; E) \delta_{qq'} \quad (4-18b)$$

Now by using above equations we get the current density function written as follows

$$\begin{aligned} j(E) &= \frac{2\pi e}{\hbar} \sum_{\mu\nu} |\langle \nu | H_B | \mu \rangle|^2 \delta(E_{\mu} - E) \delta(E_{\nu} - E) \\ &= \frac{2\pi e}{\hbar} \sum_{\mu\nu} \sum_{kk'} \sum_{qq'} \langle q | H_B | k \rangle \langle k' | H_B | q' \rangle \\ &\quad c_{q\nu}^{\dagger} c_{q'\nu} c_{k'\mu}^{\dagger} c_{k\mu} \delta(E_{\mu} - E) \delta(E_{\nu} - E) \\ &= \frac{2e}{\pi\hbar} \sum_{kk'} \sum_{qq'} T_{qk} T_{q'k'}^{\dagger} \text{Im} G_L(q'q; E) \text{Im} G_R(kk'; E) \quad (4-19) \end{aligned}$$

In this formula we see that the effect of interactions is included in the Green functions and the tunneling can take place in the bare particle representation as was shown by Appelbaum and Brinkman.<sup>33)</sup> Thus tunneling between many body states is reduced to that in the bare particle configuration, and our problem is to calculate the transfer matrix and the Green function.

Equation (4-19) is similar to the formula given by Duke,<sup>41)</sup> but our theory developed here is much simpler. We have neglected such interactions as with phonons<sup>37)</sup> or exciton,<sup>133)</sup> which will be easily contained by extending the Hamiltonians. The electron-electron interaction was also excluded in the Hamiltonians. But in deriving Eq.(4-19) we have no assumptions on the nature of  $(H_{\alpha} - H_{\alpha}^0)$ , therefore as far as the approximation of the independent electrode is satisfied we may use Eq.(4-19) for any kind of interaction.

#### § 4 - 2 Current Formula for Short Range Potential

In the previous section tunneling was formulated quite generally. Our purpose is to study the tunneling phenomena into the impurity band. In this section equation (4-19) is evaluated explicitly for a model potential,

and the current-voltage characteristics are showed to be a direct reflection of  $\text{Im } \Sigma$ , and one of the faults of our previous results Eq.(3-48) will be recovered.

As was done in Sec.3-2, in order to simplify the problem we assume that in the left hand side electrode there is no impurity and electronic state is expressed by plane wave with effective mass  $m_L$ , and electrons transfer into the right hand side electrode in which electrons travel interacting with impurity potential. Then we can reduce Eq.(4-19) to a simpler formula

$$j(E) = \frac{2e}{\hbar} \sum_{kk'} \sum_{qq'} T_{qk} T_{q'k'}^\dagger \delta_{qq'} \delta(E_q - E) \text{Im} G_R(kk'; E) \quad (4-20)$$

We assume further that the impurity potential  $v_R(r - R_n)$  in Eq.(4-2) is of short range and approximated by a  $\delta$ -well potential. Then we get the Green function of the form<sup>112)</sup>

$$G_R(kk'; E) = \frac{1}{E - \epsilon_k - \Sigma(E)} \delta_{kk'} \quad (4-21)$$

Equation (4-20) is then written as

$$j(E) = \frac{2e}{\hbar} \sum_k \sum_q |T_{qk}|^2 \delta(E_q - E) \text{Im} G_R(kk; E) \quad (4-22)$$

As was shown by Bardeen<sup>47)</sup> the vertex function is given by

$$T_{qk} = \frac{\hbar^2}{2m_B} \int \left( f_q \frac{\partial f_k^*}{\partial z} - f_k^* \frac{\partial f_q}{\partial z} \right) dS_B \quad (4-23)$$

where  $m_B$  is the reduced mass

$$\frac{1}{m_B} = \frac{1}{m_L} + \frac{1}{m_R} \quad (4-24)$$

and the surface integral should be completed in a plane parallel to the junction plane in the barrier.  $f_q$  and  $f_k$  are, respectively, solutions of the left and right hand side Schrödinger equations,<sup>132,134)</sup>

$$\left[ -\frac{\hbar^2}{2m_L} \nabla^2 + v_B(z) \theta(z - z_L) - \epsilon_q \right] f_q(r) = 0 \quad (4-25)$$

$$\left[ -\frac{\hbar^2}{2m_R} \nabla^2 + v_\phi(z) \theta(z_R - z) - \epsilon_k \right] f_k(r) = 0 \quad (4-26)$$



where  $\theta(z)$  is the step function. As was shown in Sec.2-2, the shape of the potential barrier will give little difference to the results and for the sake of simplicity we assume that  $V_B(z)$  and  $V_\phi(z)$  are a constant, i.e., a rectangular barrier. Then the vertex function is derived straight forwardly and given by

$$T_{qk} = \frac{\hbar^2}{2m_B} \delta_{q_\perp k_\perp} \kappa \frac{4 \frac{iq_\parallel}{m_L} \frac{ik_\parallel}{m_R}}{\left( \frac{iq_\parallel}{m_L} - \frac{\kappa}{m_B} \right) \left( \frac{\kappa}{m_B} - \frac{ik_\parallel}{m_R} \right)} e^{-\kappa w}, \quad (4-27)$$

where the suffices  $\perp$  and  $\parallel$  for  $q$  and  $k$  mean the vector component parallel and perpendicular to the junction plane, respectively, and  $w$  is the barrier width ( $w = z_R - z_L$ ). The penetration factor  $\kappa$  is given by

$$\kappa = \frac{1}{\hbar} \sqrt{2m_B (V_B - \varepsilon_{q_\parallel} - V)}, \quad (4-28)$$

where

$$\varepsilon_{q_\parallel} = \frac{\hbar^2 q_\parallel^2}{2m_B}. \quad (4-29)$$

Substituting Eq.(4-27) into (4-22) we get

$$j(E) = - \sum_{qk} \frac{8e\hbar^3}{m_B^2} \kappa^2 \frac{\left( \frac{q_\parallel k_\parallel}{m_L m_R} \right)^2}{\left( \frac{q_\parallel^2}{m_L^2} + \frac{\kappa^2}{m_B^2} \right) \left( \frac{k_\parallel^2}{m_R^2} + \frac{\kappa^2}{m_B^2} \right)} e^{-2\kappa w} \cdot \delta_{q_\perp k_\perp} \cdot \delta(E_q - E) \cdot \text{Im} G_R(kk; E). \quad (4-30)$$

If the barrier height is sufficiently large, which is often the actual case, the exponent in Eq.(4-30) can be approximated as

$$2\kappa w \longrightarrow \lambda + \frac{\varepsilon_\perp}{E_0}, \quad (4-31)$$

where

$$\lambda = 2 \kappa_o w = 2 \sqrt{2m_B (V_B - E - V)} / \hbar^2 w, \quad (4-32)$$

$$\varepsilon_{\perp} = \frac{\hbar^2 q_{\perp}^2}{2m_R} = \frac{\hbar^2 k_{\perp}^2}{2m_R}, \quad (4-33)$$

and

$$\frac{1}{E_o} = \frac{(2m_B)^{\frac{1}{2}}}{\hbar} (V_B - E - V)^{-\frac{1}{2}} \cdot \frac{m_R}{m_B} w. \quad (4-34)$$

Though above formulation was done for a rectangular barrier,  $\lambda$  and  $1/E_o$  can be replaced by Eqs.(2-40) and (2-41), respectively, for an abrupt p-n junction.

As we have assumed that the electronic state in the left hand side electrode is metallic, we can safely approximate  $q_{\parallel}$  by

$$q_{\parallel} = \frac{\sqrt{2m_L \varepsilon_{qz}}}{\hbar} \approx q_F, \quad (4-35)$$

where  $q_F$  is the Fermi momentum. Thus integrating Eq.(4-30) over  $q_{\parallel}$  we get

$$j(E) = -\frac{8e\hbar}{m_B^2} \kappa_o^2 \cdot \frac{\frac{q_F}{m_L}}{\frac{q_F^2}{m_L^2} + \frac{\kappa_o^2}{m_B^2}} e^{-\lambda} K, \quad (4-36)$$

where  $K$  is given by

$$\begin{aligned} K &= \sum_k \frac{(k_{\parallel}/m_R)^2}{(k_{\parallel}/m_R)^2 + (\kappa_o/m_B)^2} \exp[-\varepsilon_{\perp}/E_o] \operatorname{Im} G_R(kk; E) \\ &= \sum_{k_{\perp}} e^{-\frac{\varepsilon_{\perp}}{E_o}} \operatorname{Im} \Sigma \sum_{k_{\parallel}} \frac{(k_{\parallel}/m_R)^2}{(k_{\parallel}/m_R)^2 + (\kappa_o/m_B)^2} \frac{1}{|E - \varepsilon_k - \Sigma|^2}. \end{aligned} \quad (4-37)$$

The summation over  $k_{\parallel}$  can be completed straight-forwardly, and the result is

$$K = - \frac{(2m_R)^{\frac{1}{2}}}{2\hbar} \int_{k_{\perp}} \exp\left[-\frac{\xi_{\perp}}{E_0}\right] \left\{ \frac{V_B^* \frac{1}{2} \text{Im} \Sigma}{|V_B^* + E - \xi_{\perp} - \Sigma|^2} + \text{Re} \frac{(E - \xi_{\perp} - \Sigma)^{\frac{1}{2}}}{V_B^* + E - \xi_{\perp} - \Sigma} \right\}, \quad (4-38)$$

where the effective barrier height is defined by

$$V_B^* = \frac{\hbar^2}{2m_R} \left( \frac{m_R^2}{m_B^2} \kappa_0^2 \right). \quad (4-39)$$

The barrier height is assumed large and we can approximate the denominator in Eq.(4-38) as

$$V_B^* + E - \xi_{\perp} - \Sigma \longrightarrow V_B^* + E - \Sigma, \quad (4-40)$$

since the terms for large  $\xi_{\perp}$  has negligible contribution to the integral because of the exponential factor in Eq.(4-38). In the case of the phenomena of tunneling into the impurity band the energy  $E$  is very small;

$$V_B^* \gg E - \Sigma, \quad (4-41)$$

so we approximate Eq.(4-38) further, and we get

$$K = - \frac{(2m_R)^{\frac{3}{2}}}{8\pi\hbar^3} \cdot V_B^* \frac{3}{2} E_0 \cdot \left\{ \text{Im} \Sigma + \frac{V_B^*}{E_0} \int d\xi_{\perp} \exp\left[-\frac{\xi_{\perp}}{E_0}\right] \text{Re} \sqrt{\frac{E - \xi_{\perp} - \Sigma}{V_B^*}} \right\}. \quad (4-42)$$

Now we get the expression for the current density

$$j(E) = C_4(E, V) e^{-\lambda} Q_3(E, V), \quad (4-43)$$

where

$$Q_3(E, V) = \text{Im} \Sigma + \frac{V_B^*}{E_0} \int d\xi_{\perp} \exp\left[-\frac{\xi_{\perp}}{E_0}\right] \text{Re} \sqrt{\frac{E - \xi_{\perp} - \Sigma}{V_B^*}}, \quad (4-44)$$

and the other energy dependent factors are compressed in  $C_4(E, V)$  which varies slowly with energy and applied bias. The suffix 3 for  $Q$  means the case for three dimensional model.

By now all of the formulation have been done for the spherical symmet-

ric three dimensional energy band. In the case of one-dimensional energy band we get similar formula by putting  $k_{\perp} = 0$  in Eq.(4-20), and the result is

$$j(E) = C_5(E, V) e^{-\lambda} Q_1(E, V) , \quad (4-45)$$

where

$$Q_1(E, V) = \text{Im} \Sigma + V_B^* \text{Re} \sqrt{\frac{E - \Sigma}{V_B^*}} . \quad (4-46)$$

If we put  $\text{Im} \Sigma \longrightarrow -0$  in Eq.(4-44), by replacing  $(E - \Sigma)$  by  $E_k$  equation (4-44) gives just the same formula as tunneling density factor  $N(E, V)$  ; Eq.(3-53). This fact proves that  $\text{Im} \Sigma$  has an important role in the tunneling phenomena in the impurity band. Similar results of the self-energy effect in tunneling have been evaluated within a quasi-particle approximation.<sup>33,135)</sup> In those case, however, the tunneling characteristics are reflected by  $\text{Re} \Sigma$  as was the case in Eq.(3-70). Our present results also include those effects, i.e., for large value of  $E$ ,  $\text{Im} \Sigma$  tends to zero and  $\text{Re} \Sigma$  reflects the second term in Eqs.(4-44) and (4-46).

The tunneling current at  $T=0$  K is given by

$$J(V, T=0) = \int_{\xi_c - V}^{\xi_c} dE j(E) , \quad (4-47)$$

where  $\xi_c$  is the Fermi energy of right hand side material. The differential conductance is

$$\frac{dJ}{dV} = j(\xi_c - V) + \int_{\xi_c - V}^{\xi_c} dE \frac{\partial j(E)}{\partial V} , \quad (4-48)$$

in which the second term is approximated by

$$- \frac{\partial \lambda}{\partial V} \int_{\xi_c - V}^{\xi_c} j(E) dE = - \frac{\partial \lambda}{\partial V} J , \quad (4-49)$$

because  $C_4(E, V)$  varies slowly with respect to applied voltage compared to  $\exp[-\lambda]$ . Thus we get

$$\frac{dJ}{dV} = j(\xi_c - V) - \frac{\partial \lambda}{\partial V} J. \quad (4-50)$$

Apparently  $J$  is so small around the band edge that the second term may often be neglected. Combining Eq.(4-44) and (4-50) we know the differential conductance should reflect the dependence of  $Q_3(E = \xi_c - V, V)$  for the first order approximation. The second derivatives of the current may be more dramatic:

$$\frac{d^2 J}{dV^2} = - \left. \frac{\partial j(E)}{\partial E} \right|_{E=\xi_c-V} + 2 \left. \frac{\partial j(E)}{\partial V} \right|_{E=\xi_c-V} + \int_{\xi_c-V}^{\xi_c} \frac{\partial^2 j(E)}{\partial V^2} dE, \quad (4-51)$$

where  $\left. \frac{\partial j(E)}{\partial E} \right|_{E=\xi}$  means that  $E = \xi$  should be substituted after the differentiation is completed. The value of second and third terms in Eq. (4-51) are less than a few percentages of the first, because the value of  $\partial j(E)/\partial V$  is two orders of magnitude smaller than that of  $\partial j(E)/\partial E$ . Therefore by neglecting these terms we get an approximate formula

$$\frac{d^2 J}{dV^2} = - \left. \frac{\partial j(E)}{\partial E} \right|_{E=\xi_c-V} = - \left. \frac{\partial Q(E, V)}{\partial E} \right|_{E=\xi_c-V}, \quad (4-52)$$

where

$$\begin{aligned} \frac{\partial Q_3}{\partial E} = & \operatorname{Im} \frac{\partial \Sigma}{\partial E} + \operatorname{Re} \left[ \frac{V_B^*}{E_0} \left\{ 1 - \frac{\partial \Sigma}{\partial E} \right\} \right. \\ & \left. \left\{ \sqrt{\frac{E - \Sigma}{V_B^*}} - \int_0^\infty \sqrt{\frac{E - \Sigma - \epsilon_\perp}{V_B^*}} \exp\left[-\frac{\epsilon_\perp}{E_0}\right] d\left(\frac{\epsilon_\perp}{E_0}\right) \right\} \right], \quad (4-53) \end{aligned}$$

or

$$\frac{\partial Q_1}{\partial E} = \operatorname{Im} \frac{\partial \Sigma}{\partial E} + \frac{1}{2} \operatorname{Re} \left[ \sqrt{\frac{V_B^*}{E - \Sigma}} \left( 1 - \frac{\partial \Sigma}{\partial E} \right) \right]. \quad (4-54)$$

In measuring the differential conductance fine structures due to the structures in the density of states of the impurity band may be weakened by the second term in Eq.(4-50). But by measuring the second derivatives of the current we can get convincing informations about the functional form of  $Q_1(E, V)$  and therefore about the energy spectrum of the impurity band.

### § 4 - 3 Numerical Investigation of the Conductance

In this section we will show numerically that the theoretical formula for the tunneling current density does reflect the density of states of the impurity band. To do this let's start with the formulation of the state density function. According to Eq.(3-23) the self-energy for the Green function is given by

$$\begin{aligned}\Sigma &= H' + H' G_0 H' + H' G_0 H' G_0 H' + \dots \\ &= H' \frac{1}{1 - G_0 H'}\end{aligned}\quad (4-55)$$

By replacing  $G_0$  by  $\langle G \rangle_{av}$  we get coupled equations for the state density function  $Z$ :

$$Z = \sum_k \langle G \rangle_{kk} = \sum_k \frac{1}{E - \epsilon_k - \Sigma(E)}, \quad (4-56)$$

and

$$\Sigma = H' \frac{1}{1 - \langle G \rangle_{av} H'} \quad (4-57)$$

The density of states  $D(E)$  is given by

$$D(E) = -\frac{1}{\pi} \text{Im } Z \quad (4-58)$$

Here we will apply the results given by Saitoh et al., who obtained a cubic equation for three dimensional crystal<sup>112,136,137)</sup>

$$\frac{E}{\epsilon_g} = \frac{\nu_3}{y} - (1 - y)^2, \quad (4-59)$$

which is equivalent to Eq.(4-56), and the state density and self-energy are related to  $y$  as

$$D(E) = \frac{N_i}{\pi \nu_3 \epsilon_g} \text{Im } y, \quad (4-60)$$

and

$$\frac{\Sigma(E)}{\varepsilon_g} = \frac{\nu_3}{y}, \quad (4-61)$$

respectively. In Eq.(4-59)  $\varepsilon_g$  is the ionization energy of single impurity and the reduced impurity concentration  $\nu_3$  is defined by

$$\nu_3 = \frac{2\pi N_1 \hbar^3}{\sqrt{2m^3 \varepsilon_g^3}}. \quad (4-62)$$

Using Eqs.(4-59) and (4-61) we can write Eqs.(4-44) and (4-53), respectively, as follows

$$\frac{Q_3}{\varepsilon_g} = \operatorname{Im} \frac{\nu_3}{y} - \left( \frac{V_B^*}{\varepsilon_g} \right)^{\frac{1}{2}} \operatorname{Im} S_3, \quad (4-63)$$

and

$$\begin{aligned} \frac{\partial Q_3}{\partial E} &= \operatorname{Im} \frac{\nu_3}{\nu_3 - 2y^2(1-y)} \\ &- \frac{\varepsilon_g}{E_0} \left( \frac{V_B^*}{\varepsilon_g} \right)^{\frac{1}{2}} \operatorname{Im} \frac{2y^2(1-y)(1-y-S_3)}{\nu_3 - 2y^2(1-y)}, \end{aligned} \quad (4-64)$$

where

$$S_3 = \int_0^\infty dt \cdot \exp[-t] \sqrt{(1-y)^2 + \frac{E_0}{\varepsilon_g} t}. \quad (4-65)$$

Similar formulae are obtained for one-dimensional model<sup>138)</sup> corresponding to Eqs.(4-59) - (4-64) as follows.

$$\frac{E}{\varepsilon_g} = - \frac{1}{x^2} - \frac{\nu_1}{1-x}. \quad (4-66)$$

$$\nu_1 = \frac{4N_1 \hbar}{\sqrt{2m \varepsilon_g}}. \quad (4-67)$$

$$D(E) = - \frac{1}{\pi U_0} \operatorname{Im} x. \quad (4-68)$$

$$\frac{\Sigma}{\epsilon_g} = - \frac{\nu_1}{1-x} \quad (4-69)$$

$$\frac{Q_1}{\epsilon_g} = - \operatorname{Im} \left( \frac{\nu_1}{1-x} \right) - \left( \frac{V_B^*}{\epsilon_g} \right)^{\frac{1}{2}} \operatorname{Im} \frac{1}{x} \quad (4-70)$$

$$\frac{\partial Q_1}{\partial E} = \operatorname{Im} \frac{\nu_1 x^3}{\nu_1 x^3 - 2(1-x)^2} + \frac{1}{2} \left( \frac{V_B^*}{\epsilon_g} \right)^{\frac{1}{2}} \operatorname{Im} \frac{2x(1-x)^2}{\nu_1 x^3 - 2(1-x)^2} \quad (4-71)$$

Computational results of above formulae are shown in Figs.(4-2) - (4-7).

By comparing those curves, the following features are demonstrated;

- (a) If the impurity concentrations is lower than the critical concentration  $\nu_c = 8/27$ , or the impurity band is separated from the main band,  $\partial Q/\partial E$  becomes infinity around the energy gap. Even if the impurity concentration is higher than  $\nu_c$ ,  $\partial Q/\partial E$  exhibits a sharp structure due to the dip of density of states.
- (b) In the impurity band region,  $Q$  and  $\partial Q/\partial E$  are dominated by the functions of  $\operatorname{Im} \Sigma$  and  $\operatorname{Im}(\partial \Sigma / \partial E)$ , respectively. According to the sharp cut-off of  $\operatorname{Im} \Sigma$  and  $D(E)$  at lower energy side of the impurity band,  $\partial Q/\partial E$  becomes infinity.
- (c) In the main band region, the curves for  $Q_3$  are different from those for  $Q_1$ . The former exhibits a linear relation, if  $E_o/\epsilon_g$  is large. If  $E_o/\epsilon_g$  small, however, it does not. In the case of one dimensional model,  $Q_1$  is dominated by the second term in Eq.(4-70) and does not reflect the one-dimensional density of states.

The characteristics shown in Figs.(4-3) - (4-5) are sensitive to the junction parameter  $E_o/\epsilon_g$ , especially if it is small. If the junction studied involves an insulator film, its thickness should be measured exactly. In the case of a semiconductor junction, the value of  $E_o$  is determined by Eq.(2-41). Practically the value of  $E_o/\epsilon_g$  is of the order of unity for many of the materials.

Before concluding this section, we will show the Sum Rule for the current as a proof of the completeness of the theory, which may be described as "If the tunneling probability is constant the tunneling current should be proportional to the electron density of an electrode". Our problem is to prove the relation



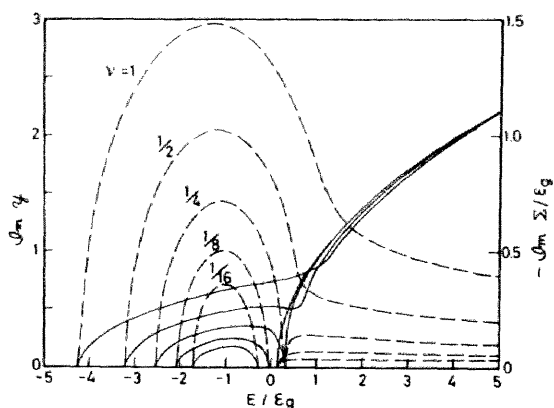


Fig. 4-2. State density function ( solid lines ) and imaginary part of the self-energy ( broken lines ) for three dimensional model. The critical concentration is  $\nu_c = 8/27$ .

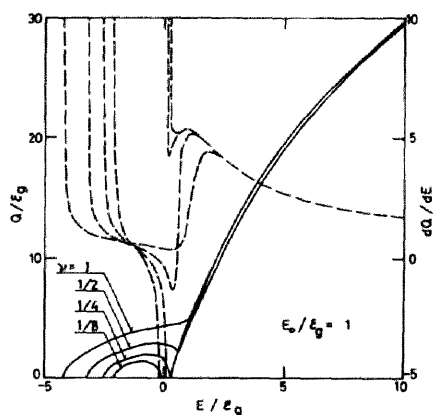


Fig. 4-3. The function of  $Q$  ( solid lines ) and  $\partial Q/\partial E$  ( broken lines ) for  $E_0/\epsilon_g = 1.0$ . The barrier height is set to be  $V_B^*/\epsilon_g = 100$ . In the main band region the curves for  $Q$  are nearly parabolic. The sharp dip of  $\partial Q/\partial E$  around the energy gap is due to  $\text{Im}\partial\Sigma/\partial E$ , and a direct reflection of the impurity band. The infinity of  $\partial Q/\partial E$  at the lower energy side of the impurity band is due to the sharp cut-off of the density of states.

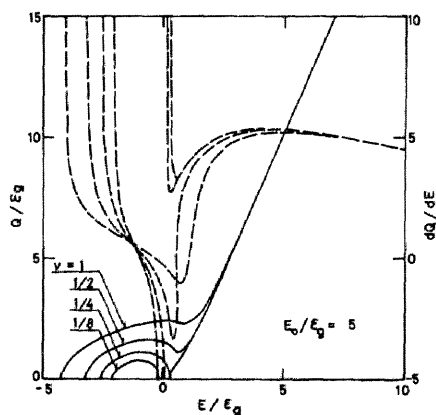


Fig. 4-4. The function of  $Q$  and  $\partial Q/\partial E$  for  $E_0/\epsilon_g = 5.0$  and  $V_B^*/\epsilon_g = 100$ . In the main band region the curves for  $Q$  exhibits linearity. They have fine structures (sharp dip ) around the energy gap.

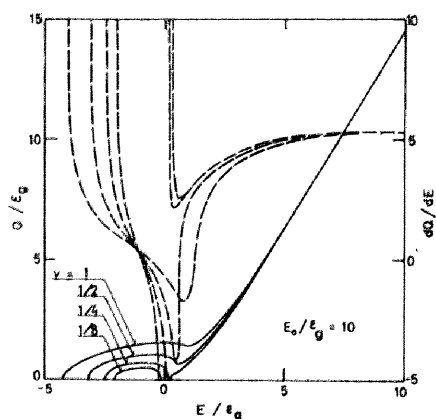


Fig. 4-5. The function of  $Q$  and  $\partial Q/\partial E$  for  $E_0/\varepsilon_g = 10.0$  and  $V_B^*/\varepsilon_g = 100$ . Curves show linearity of  $Q$  in the wider range of the main band region. The dips around the gap are enhanced.

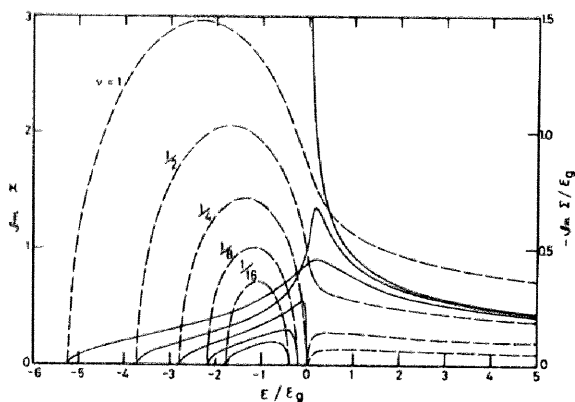


Fig. 4-6. State density function (solid lines) and imaginary part of self-energy (broken lines) for one dimensional model. The critical concentration is  $\nu_c = 8/27$ .

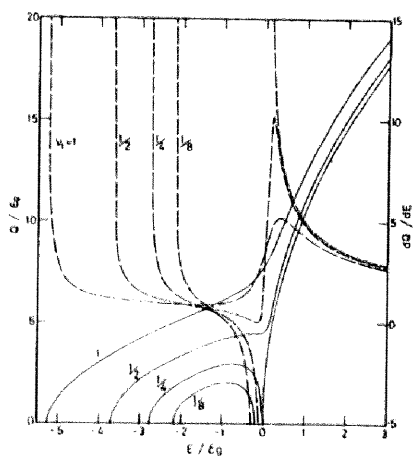


Fig. 4-7. The functions  $Q$  (solid lines) and  $\partial Q/\partial E$  (broken lines) for one dimensional model. This is a limiting case of the three dimensional model, say  $E_0/\varepsilon_g \rightarrow +0$ . In the main band region  $Q$  is inversely proportional to the state density.

$$J(V, T=0) = CN_i, \quad (4-72)$$

where  $C$  is a constant. Combining Eqs.(4-8), (4-43) and (4-63) we get the following integral:

$$J(V, T=0) = \beta \int_{-\infty}^{\xi_c/\epsilon_g} dw \left( \operatorname{Im} \frac{\nu_3}{y} - \frac{V_B^*}{\epsilon_g} \operatorname{Im} S_3 \right), \quad (4-73)$$

where  $\beta$  is a constant and  $w$  is the dimensionless energy  $w = E/\epsilon_g$ . By using the relation

$$\operatorname{Im} \chi(w) = \frac{1}{2i} \left\{ \chi(w + i\delta) - \chi(w - i\delta) \right\}, \quad (4-74)$$

the integration over  $w$  should be performed on the path  $\Gamma$  in the complex  $w$ -plane as shown in Fig.(4-8a),

$$J(V, T=0) = \frac{\beta}{2i} \int_{\Gamma} dw \left\{ \frac{\nu_3}{y} - \sqrt{\frac{V_B^*}{\epsilon_g}} S_3 \right\} \quad (4-75)$$

This integral is evaluated by converting the integral to that in the  $y$ -plane, the corresponding path  $\Gamma'$  is also shown in Fig.(4-8b).

$$\begin{aligned} J(V, T=0) &= \frac{\beta}{2i} \int_{\Gamma'} dy \frac{dw}{dy} \left\{ \frac{\nu_3}{y} - \sqrt{\frac{V_B^*}{\epsilon_g}} S_3 \right\} \\ &= \beta \pi \nu_3 \left\{ 2 + \sqrt{\frac{V_B^*}{\epsilon_g}} \int_0^{\infty} \left( 1 + \frac{E_0}{\epsilon_g} t \right)^{-\frac{1}{2}} e^{-t} dt \right\} \\ &\quad + \beta \nu_3 \operatorname{Im} \left\{ \frac{\nu_3}{2y^2} - 2 \ln(y) + 2y - \sqrt{\frac{V_B^*}{\epsilon_g}} \int_0^{\infty} dt e^{-t} Y(y) \right\}, \quad (4-76) \end{aligned}$$

where

$$Y(y) = \frac{1}{y} \sqrt{(1-y)^2 + \frac{E_0}{\epsilon_g} t}$$

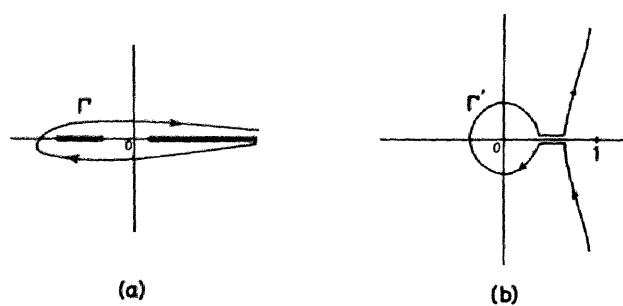


Fig. 4-8. (a) The integral path in  $w$ -plane.  
(b) The integral path in  $y$ -plane.

$$\begin{aligned}
& + \frac{1}{\sqrt{1 + \frac{E_0}{\epsilon_g} t}} \ln \frac{\sqrt{(1-y)^2 + \frac{E_0}{\epsilon_g} t} - \sqrt{1 + \frac{E_0}{\epsilon_g} t} - y}{\sqrt{(1-y)^2 + \frac{E_0}{\epsilon_g} t} + \sqrt{1 + \frac{E_0}{\epsilon_g} t} - y} \\
& + \ln \left\{ 1 - y + \sqrt{(1-y)^2 + \frac{E_0}{\epsilon_g} t} \right\} + \frac{2}{3 \nu_3} \left\{ (1-y)^2 + \frac{E_0}{\epsilon_g} t \right\}^{\frac{3}{2}} . \quad (4-77)
\end{aligned}$$

The value of  $y$  should be chosen so as to give the value for the Fermi energy, and if it falls in the energy gap we see that  $\text{Im } y = 0$ . Consequently the second term in Eq.(4-76) equals to zero and we get

$$J(V, T=0) = \nu_3 \beta \pi \left\{ 2 + \sqrt{\frac{V_B^*}{\epsilon_g}} \int_0^\infty \left( 1 + \frac{E_0}{\epsilon_g} t \right)^{-\frac{1}{2}} e^{-t} dt \right\} , \quad (4-78)$$

which is the formula required and we have concluded the proof.

#### § 4 - 4 Experimental Considerations

About the sample described in Sec.3-3, the measurements of the second derivatives were done at liq.He temperature. In the measuring circuits the second harmonics involve the trace of the  $(dV/dJ)^3 (d^2J/dV^2) - V$  curves, where  $J$  is the sum of the direct and indirect current components.<sup>126)</sup> Thus the large indirect current component makes it difficult to measure the second derivatives of the direct current component so accurately as to be comparable with the theoretical curves. So we obtained  $d^2J/dV^2 - V$  curves for the direct current component by calculating numerically with the aid of the  $dJ/dV - V$  plots. Figure (4-9) is one of the typical  $d^2J/dV^2 - V$  plots for an As doped germanium tunnel junction. In the higher energy region the curves are nearly constant reflecting the linearity of  $dJ/dV - V$  curves. Around the band edge there exists a sharp dip, which is the evidence for the dip of the state density between the impurity band and the main band.

The similar measurements were made on Sb doped samples; the results

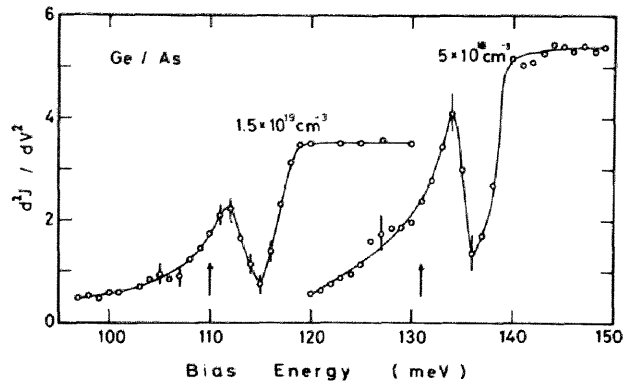


Fig. 4-9. Typical conductance plots at 4.2 K for As doped samples. The sharp dip in the middle energy region proves the dip in the density of states. The arrows show the energy corresponding to the edge of the main band with parabolic dependence.

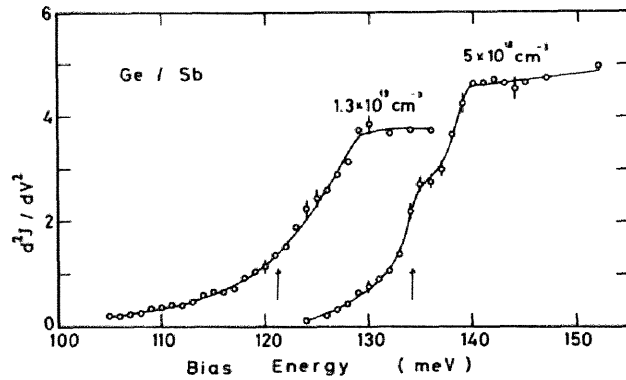


Fig. 4-10. Typical conductance plots at 4.2 K for Sb doped samples. There are no indication of the dip in the curves within the experimental error.

are shown in Fig.(4-10). The curve for a lower donor concentration seems to have a small convex in a middle energy region, but that for a higher concentration have no indication within the experimental error. In the lower energy region curves for both samples show long tail, suggesting that the impurity band decays continuously into the forbidden band in contrast to the theoretical results. In what follows we will discuss the results about three regions separately.

(a) Higher energy region ( Main band )

According to the numerical considerations in Sec.4-3, the characteristics for the main band region is sensitive to the junction parameter. By using the values for the direct current component in germanium:<sup>127)</sup>  $V_B = 0.9$  eV,  $m_R = 0.04 m_0$  and  $\epsilon = 16$ , the value of  $E_o = 0.02$  eV is estimated for  $N_d = 5 \times 10^{18} \text{ cm}^{-3}$  and  $E_o = 0.05$  eV for  $1.5 \times 10^{19} \text{ cm}^{-3}$ , in a bias voltage region measured ( $100 \text{ meV} < -V < 150 \text{ meV}$ ). As the ionization energy of (111) valleys are 0.0127 eV (As) and 0.0096 eV (Sb),<sup>60)</sup> within the effective mass approximation the 1S hydrogenic energy for (000) valley are 0.0029 eV (As) and 0.0022 eV (Sb). Therefore the junction parameter  $E_o/\epsilon_g$  are estimated to be about 7 (As) and 9 (Sb) for the samples of  $N_d = 5 \times 10^{18} \text{ cm}^{-3}$  and larger for samples of higher concentrations. Thus the value of  $E_o/\epsilon_g$  is large enough for the curve of Q to exhibit the linearity, and the agreement of the experimental results proves the parabolicity of the energy band in the higher energy region.

(b) Middle energy region ( Energy gap )

The sharp dip for an As doped sample Fig.(4-8) is the evidence of the existence of the dip of the density of states between the impurity band and the main band, which proves the reasonableness of Fig.(3-7). The fact that there is no evidence of the dip for Sb doped samples suggests that the impurity concentration is high, i.e., the sample is in the metallic region. By using the  $\delta$ -well potential for  $v(r - R_n)$  the critical concentration  $N_c$  at which the impurity band merges into the main band is given by<sup>112)</sup>

$$N_c = \frac{\sqrt{32 m_R^3 \epsilon_g^3}}{27 \pi \hbar^3} \quad (4-79)$$

The value of  $N_c$  for As and Sb donors in germanium are  $N_c(\text{As}) = 4.5 \times 10^{17} \text{ cm}^{-3}$  and  $N_c(\text{Sb}) = 3 \times 10^{17} \text{ cm}^{-3}$ , respectively. Both values differ

only slightly and cannot explain the difference between a Sb doped sample and As doped one. But the theory does not take into account the long range nature of the atomic potentials. A Sb atom should have larger effective range of the potential because of its larger atomic radius<sup>56)</sup> and it should have a smaller value of  $N_c$  than As atom has. In measuring the electric and electronic properties Sb doped samples often exhibit different characteristics from As doped samples,<sup>73)</sup> and they are in good agreement with our present result. For example, Yamanouchi measured the Hall coefficient of germanium and found that Sb doped sample exhibits the evidence of the degenerate free electron gas ( $N_d \geq 10^{17} \text{ cm}^{-3}$ ) while As doped one is not explained by the free electron model.<sup>139-142)</sup>

#### (c) Lower energy region (Band tail)

Figure (4-11) shows the semi-log plots of the second derivatives in the lower energy region. Each curve is quite similar to that of density of states Fig.(3-8), and shows the band tail extending continuously into the forbidden band, differing from the theoretical results: Figs.(4-2)-(4-6). Bonch-Bruевич<sup>81)</sup> showed theoretically that the impurity band has long tail within the first order approximation, if the potential is of the long range type. Similar results have been obtained by Kanda-Onodera<sup>143)</sup> and Kanda-Hasegawa.<sup>144)</sup> Though there are many assumptions and approximations adopted in their theories, it seems true that the long range nature of the impurity potential will reflect directly the long tail.<sup>145)</sup> By using the screened Coulomb potential, the effects of the formation of clusters in impurity distribution was studied by Kane<sup>146)</sup> and Halperin-Lax.<sup>71)</sup> The latter gave the density of states in the high density limit (metallic concentration region) of the form expressed by Eq.(3-57). The results for Sb doped samples are in good agreement with their theory, suggesting that Sb is easier to form clusters due to large atomic radius.<sup>147,148)</sup>

By comparing Fig.(3-7a) with (3-7b), we know that the impurity band for As doped sample is much larger than that for Sb doped one. Why? Cuevas and Fritzsche<sup>149,150)</sup> determined the value of strain at which the saturation of the piezo-resistance occurs and found roughly agreement for Sb doped germanium with what would be expected with parabolic band. But in the case of As doped sample the results couldn't be understood without the assumption of the presence of large tail states. Their results have been attributed to the significance of the large central impurity cell potential of As donors.<sup>151)</sup> The central cell correction has also been thought to be



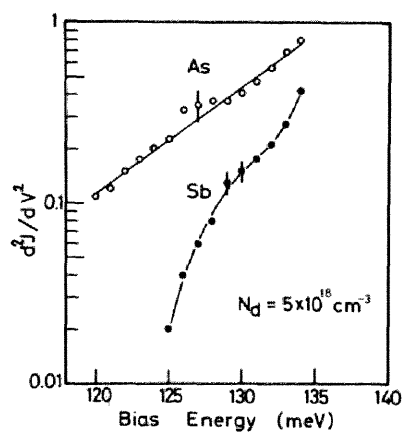


Fig. 4-11. The  $d^2J/dV^2 - V$  curves for the band tail region. The curve for an As doped sample shows a linearity, but that for a Sb doped one does not. ( See Fig. 3-8. )

responsible for the mixing of the electronic states of (000) valley with those of (111) valleys, giving larger impurity induced tunneling current to a tunnel diode made of As doped germanium.<sup>22)</sup> Thus our present results for impurity band of (000) valley may also be attributed to the larger central impurity cell potential in an As doped sample.

Kaplan<sup>152)</sup> investigated the impurity level for subsidiary valley in the framework of the effective-mass theory by Kohn<sup>60)</sup> and showed that if the impurity potential is of the screened Coulomb type there are hydrogen-like localized states near the subsidiary minimum, while for the impurity potential of  $\delta$ -well type it has no localized states. Similar results have been obtained by Peterson.<sup>153)</sup> Present results are the first observation of the impurity level associated with (000) subsidiary valley of germanium, and another proof of the long range nature of the impurity potentials. Further experiments by introducing any other impurities or by applying deformation may be of value for the examination of the effective-mass theory for a many valley semiconductor.<sup>154)</sup>

## V. LOCALIZATION AND DENSITY OF STATES

### § 5 - 1 Magnetic Moment in Tunnel Diode

The electronic states in the impurity band ( or band tail ) will have the localized nature, irrespective to the concentration of donor ( or acceptor ) impurities.<sup>155-157)</sup> As is illustrated in Fig.5-1, electrons in doped semiconductors should have both localized and non-localized nature. The matter is, therefore, which nature dominates the phenomena considered.

The negative magneto-resistance observed in a heavily doped semiconductor at very low temperature has been thought to be a reflection of the localized nature of electrons.<sup>158)</sup> Toyozawa<sup>78)</sup> investigated the co-operative effect of electron correlation and the random lattice. He showed that the localized magnetic moment should appear as a collective mode and concluded that the negative magneto-resistance has its origin on the localized moment. Similar phenomena in a ferromagnetic metal was studied by Yamada and Takada,<sup>159)</sup> attributing the negative magneto-resistance to spin fluctuations. Thus the immobile state in the impurity band is thought to be responsible for the anomalous electrical conduction in a heavily doped semiconductor. In this chapter we will further study the localized nature of electrons by measuring the zero bias conductance anomaly ( ZBA ) in tunnel diodes.

Among many types of ZBA observed in the low temperature characteristics of a tunnel junction, the conductance maximum sensitive to temperature is due to the magnetic scattering.<sup>32,77,160)</sup> Appelbaum<sup>32)</sup> and Solyom-Zawadowski<sup>161)</sup> studied the strong coupling limit of Kondo scattering in a tunnel junction and concluded that for an anti-ferromagnetic coupling  $\Delta G$  is maximum when the interaction is  $T_j$  dominant and  $\Delta G$  is minimum with a sharp maximum due to strong coupling when it is  $T_a$  dominant ( See Fig.5-2 ), where the matrix element  $T_a$  corresponds to the impurity assisted non-magnetic tunneling in a magnetic barrier and  $T_j$  to the magnetic



Fig. 5-1. The electronic states in the impurity band may be described by atomic wave functions and should have localized nature, while electrons in the main band behave like free electrons. At a finite temperature electronic properties should reflect both features.

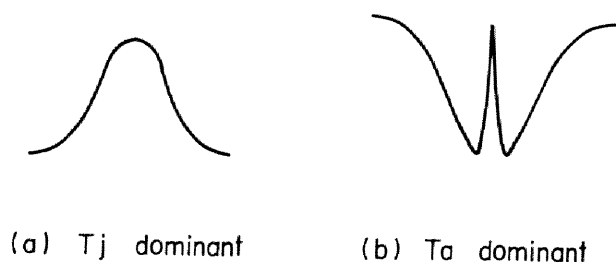


Fig. 5-2. The ZBA for an anti-ferromagnetic coupling exhibits two types of conductance.  $\Delta G$  is maximum for  $T_j$  dominant case (a), or minimum with narrow maximum for  $T_a$  dominant case (b).

tunneling with spin flip.

## § 5 - 2 Experimentals

Measurements were done at low temperature (  $1.6 < T < 30 \text{ K}$  ) about the tunnel diodes made by the same method described in §3-3. In an As doped germanium tunnel junction  $\Delta G$  was always maximum and had the characteristics of Kondo scattering for  $T_j$  dominant case. In the case of a Sb doped sample there was no indication of ZBA due to Kondo scattering. Figure 5-3 is the typical curves of  $dV/dI - V$  at 4.2 K, in which we can see the zero bias resistance minimum or the conductance maximum for As doped sample. Other structures above 8 meV are due to the emission of the zone boundary TA, LA, LO and TO phonons.<sup>162)</sup> At higher temperatures the structure around zero-bias becomes less prominent and finally disappears at about  $T_0 = 20 \text{ K}$ . This temperature sensitive part is called the ZBA.

The ZBA of As doped sample are shown in Fig.5-4 for various temperatures by using the differential conductance. Raising the temperature the line shape becomes more asymmetric. The maximum value of  $\Delta G/G_0$  is plotted in Fig.5-5 as a function of temperature. In a higher temperature region the  $\Delta G/G_0$  is proportional to  $\ln T$ , which is one of the characteristic nature of ZBA predicted by Appelbaum. In a lower temperature region the curve deviates from the linear dependence due to strong coupling, indicating that the sign of the exchange energy  $J$  must be negative, or the coupling is anti-ferromagnetic.

According to the theory by Appelbaum<sup>32)</sup>  $\Delta G$  for  $T_j$  dominant case is given as follows; for a weak coupling or at high temperature region,

$$\frac{\Delta G}{G_0} \sim N_s J \rho_F F(\text{eV}, T) , \quad (5-1)$$

where  $\rho_F$  is the density of states of electron at the Fermi-level in a magnetic material,  $N_s$  the number density of magnetic spin and  $J$  is the exchange energy.  $F(\text{eV}, T)$  is

$$F(eV, T) = \iint \frac{\partial f(w + eV)}{\partial w} \frac{\partial f(w')}{\partial w'} \ln \left| \frac{w - w'}{D} \right| dw dw', \quad (5-2)$$

where  $f(w)$  is the Fermi-Dirac distribution function and  $D$  is the cut-off parameter. For a strong coupling case or at low temperature limit,

$$\frac{\Delta G}{G_0} \sim N_s \frac{1}{(J \rho_F)^2} \frac{\Delta_0^2}{(eV)^2 + \Delta_0^2}, \quad (5-3)$$

where  $\Delta_0$  is the characteristic energy of scattering at  $T=0$  K. Equation (5-2) exhibits the characteristic  $\ln T$  dependence at high temperature and  $\ln|eV|$  dependence at high energy. By measuring the temperature at which  $\Delta G/G_0$  deviates from  $\ln T$  dependence we can estimate the value of  $\Delta_0$ ; <sup>165)</sup> the results are summarized in Tab.5-1. According to the theory by Nagaoka <sup>166)</sup> the characteristic energy is given by

$$\Delta_0 = D \exp \left[ - \frac{1}{2J \rho_F} \right], \quad (5-4)$$

showing that if the impurity concentration is large  $\rho_F$  is large and accordingly  $\Delta_0$  should be large in good agreement with the experimental results. The magnitude of  $\Delta G/G_0$  is larger for a sample of lower concentrations, showing that the lower the donor concentration is the larger the number density of the localized spin is, which is in good agreement with Toyozawa's prediction. <sup>78)</sup>

Applying a magnetic field up to 15 KOe, the effect was so small as to be detected only in the second derivatives of the current. To confirm the mechanism we introduced Mn atoms into the junction by alloying In-Ga-Mn (Ga 0.5%, Mn 1%). The results are shown in Fig.5-6. The ZBA was enhanced showing that Mn is magnetic in germanium. As the donor concentration of the sample is  $1.5 \times 10^{19} \text{ cm}^{-3}$ , and the solubility of Mn is expected to be less than  $10^{16} \text{ cm}^{-3}$ , <sup>163)</sup> so the compensation effect can be neglected. Assuming additive nature of the conductance (Note that the tunneling is formulated within the linear response approximation), the component due to Mn atoms is obtained as the difference between the two curves in Fig.5-6; the result is shown in Fig.5-7. The component is also characteristic to the magnetic scattering. The characteristic energy for this component is too low to be measured. The low value of  $\Delta_0$  for Mn

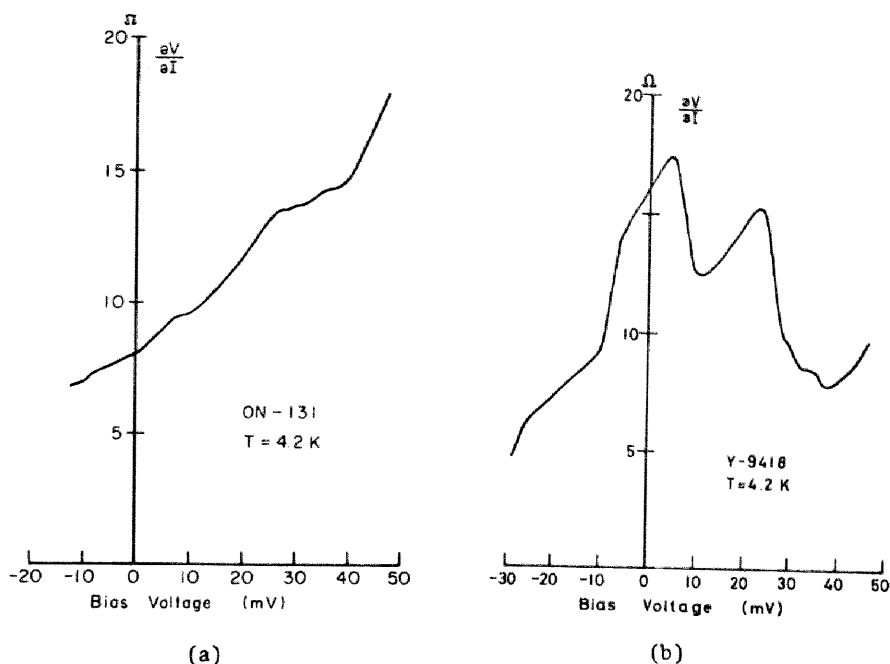


Fig. 5-3. Typical  $dV/dI - V$  curve for an As doped germanium tunnel diode (a) and a Sb doped one (b). The ZBA for an As doped sample is a resistance minimum. In the case of Sb doped sample there is no indication of ZBA.

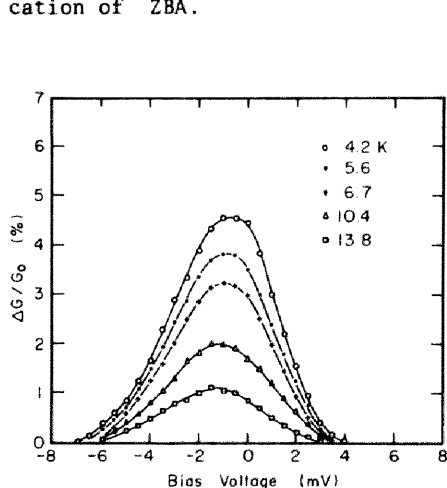


Fig. 5-4. Energy dependence of ZBA for various temperatures. In the higher energy region they show characteristic  $\ln|eV|$  dependence. ( $N_d = 5 \times 10^{18} \text{ cm}^{-3}$ )

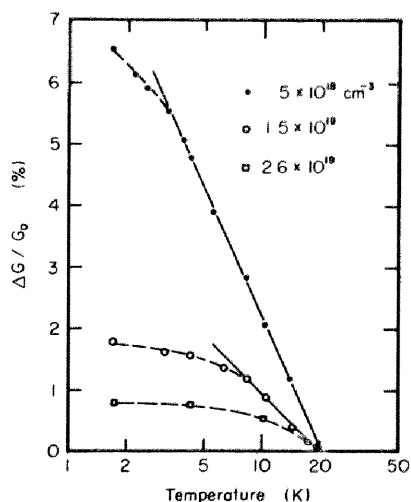


Fig. 5-5. Temperature dependence of ZBA for various donor concentrations. In the lower temperature the curves deviate from linearity, characteristic to the strong coupling.

Table 5-1. Properties of magnetic scattering. For the sake of comparison previous results for GaAs and Si are tabulated.

Sample		$\Delta G/G_o$ (T = 4.2 K)	T <sub>o</sub>	$\Delta_o$
As	$5 \times 10^{18} \text{ cm}^{-3}$	$4.8 \pm 0.3 \%$	$20 \pm 2 \text{ K}$	$0.33 \pm 0.04 \text{ meV}$
	$1.5 \times 10^{19}$	$1.5 \pm 0.2$	$20 \pm 3$	$0.72 \pm 0.07$
	$2.6 \times 10^{19}$	$0.7 \pm 0.2$	$\sim 20$	$0.8 <$
	Mn	$0.7 \pm 0.2$	$\sim 20$	?
Sb	$5 \times 10^{18}$	No		
	$1.3 \times 10^{19}$			
GaAs *			$\sim 55$	$0.6 \pm 0.2$
Si ( P-doped ) **			$\sim 10$	$\sim 0.053$

\* N.A. Mora, M. Kuhn and J.J. Loferski : Proc. Intern. Conf. Physics of Semiconductors, Moscow, 1968, p.274.

\*\* D.L. Losee and E.L. Wolf : Ref. 36.



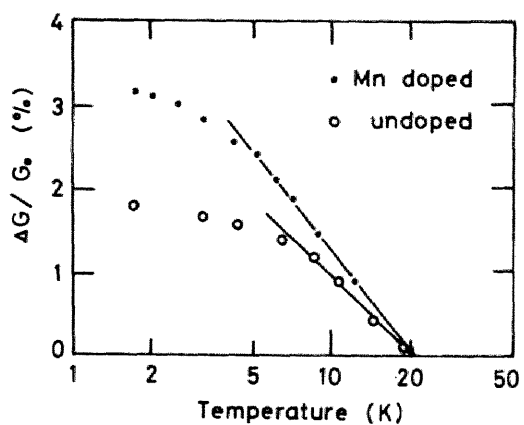


Fig. 5-6. By introducing Mn into the junction, the ZBA is enhanced. The donor concentration of the sample is  $1.5 \times 10^{19} \text{ cm}^{-3}$ .

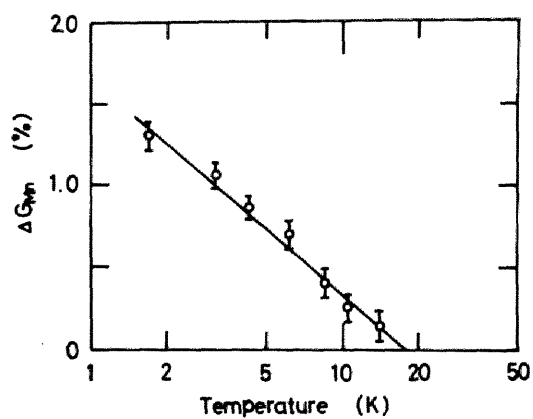


Fig. 5-7. The anomalous conductance due to Mn atoms. It exhibits  $\ln T$  relation characteristic to the weak coupling of Kondo scattering.

suggests that the coupling constant  $J$  is much smaller than that for the localized moment existing intrinsically in a heavily doped germanium. The fact that the magnitude of  $\Delta G/G_0$  for sample of  $N_d = 2.6 \times 10^{19} \text{ cm}^{-3}$  due to the intrinsic magnetic moment is nearly equal to that due to extrinsic Mn impurities indicates that the number density of intrinsic moment is of the order of  $10^{16} \text{ cm}^{-3}$  for this sample. The sample of  $N_d = 5 \times 10^{18} \text{ cm}^{-3}$  is expected to have an order of magnitude larger number of localized spin. This is a reasonable value because Toyozawa estimated the number ratio of the electron with localized spin to the non-magnetic electron as less than ten percents.

### § 5 - 3 Localized Spin and Density of States

We have ever seen that an As doped germanium has localized moment as well as the indication of the impurity band, while a Sb doped one has no localized moment and its impurity band is completely merged into the main band. This fact proves earlier expectations that the localized spin is closely related to the impurity band.<sup>158)</sup> Because the results in Sec.3-3 and Sec.4-4 are for the subsidiary valley while those in Sec.5-2 are for the (111) main band valley, we'll restrict ourselves to the qualitative discussions in this section.

As was already mentioned the electronic state in the impurity band should be essentially localized, and the delocalized nature may come out from the overlapping of the atomic wave functions. The distribution of the impurity atoms is at random, that is, the degree of the overlapping should be different from site to site. In other words, the material is microscopically inhomogeneous, which is the origin of the magnetic moment showed by Toyozawa.<sup>78)</sup> Therefore we may find some localized states somewhere in the crystal, even in the highly doped material. If the impurity band is merged into the main band, some of the electrons behave as free-electrons in the conduction band extending over the whole crystal, which have somewhat different natures from the delocalized states in the impurity band. Thus in a heavily

doped semiconductor electronic states should have at once both localized and non-localized nature, or in a quantum mechanical term the electronic wave function should be described by some combinations of plane waves and atomic wave functions.

By the way, most of the properties associated with electronic conduction are dominated by the electrons near the Fermi level,<sup>54)</sup> which is determined so as to satisfy the following relation:

$$n_o = 2 \int_0^{z_F} D(E) dE \quad , \quad (5-5)$$

where  $n_o$  is the total number density of electrons ( nearly equals to  $N_d$  ) and the factor 2 comes from the spin degeneracy. If the impurity band is separated from the main band, the Fermi level should lie in the impurity band. If the impurity band is merged into the main band, it is somewhere near the main band edge, and in this case the electric properties should reflect both natures of the impurity band and the main band.

The dip of the density of states observed in an As doped sample suggests that the Fermi level falls in the vicinity of the dip and the electronic conduction should reflect the nature of the impurity band. In the case of a Sb doped sample the Fermi level is expected to lie in the main band, or the electronic properties are dominated by the conduction electrons. Though we have not known the evidence of the impurity band for the (111) valleys, it seems reasonable to expect similar density of states to that of (000) valley, and what mentioned above is thought to be the reason why we cannot find magnetic moment in a Sb doped sample. The number ratio of the electron with localized spin to the non-magnetic electron seems in good agreement with Toyozawa's estimations, suggesting that the localized moment does appear as the collective mode of many electron system.<sup>136)</sup>

Theory of tunneling into impurity band of a heavily doped semiconductor was developed in the frame work of CPA. First, the tunneling probability for a semiconductor p-n junction was investigated in an exact formula and the expression for the current was found to include the density of states factor which is a function of the density of states of both electrodes. On the basis of the wave function for the impure semiconductor, the current formula was analyzed which gave the method of determining the density of state tail through tunneling measurements. Secondly, the nature of the tunneling current into the impurity band was investigated in the framework of the Hamiltonian formalism with the aid of Green Function method. The tunneling current was given as a function of the electronic self-energy. The first and second derivatives of the current with respect to applied voltage were found to give informations of the energy gap between the impurity band and the main band. In the impurity band the  $dJ/dV - V$  curve reflects the influence of  $\text{Im } \Sigma$ , while in the main band region it reflects the parabolic behaviour of the density of states.

Using the formula given above, the energy spectra of impurity band of (000) valley of germanium doped with As and Sb donors were investigated. An impurity band was found for an As doped germanium, while in the case of a Sb doped sample the impurity band was merged completely into the main band showing that the sample is in the metallic region. The energy dependence of the density of states of the impurity band tail was nearly exponential extending continuously into the forbidden band for both samples, reflecting the long range nature of the impurity potential. The results are the first observation of the localized states associated with (000) subsidiary valley of germanium.

Anomalous zero-bias conductance maximum was found for a tunnel diode made of As doped germanium, characteristic to the magnetic Kondo scattering. The mechanism was confirmed by introducing Mn into the junction, and the nature of the magnetic moment in the impurity band was

discussed. The exchange energy was negative and larger than that for d-electron of Mn. The results were in good agreement with the theory by Toyozawa, and impurity band was proved to be the origin of the localized spin in a degenerate semiconductor.

Several problems remain. The experimental results for impurity band decays exponentially into the forbidden band, which cannot be explained by the present theories. The general formula including off-diagonal terms has not been evaluated, which will be of great use to investigate the shape of the impurity potential. The results were about the (000) subsidiary valley, it is desirable to investigate phenomena appeared in connection with the lowest valley. In order to estimate the effect of formation of clusters, further studies for sample of much wider range of donor concentration are valuable. The compensation of the sample by irradiation or other means may be of value.

## ACKNOWLEDGEMENTS

The author wishes to thank his advisor, Professor Tetsuya Arizumi for his advice, guidance and support throughout the course of the research.

He is indebted to Dr. Akira Yoshida who made the initial tunneling measurements and developed many of the experimental techniques.

He wishes to thank Professor Masayuki Ieda and Dr. Tatau Nishinaga for their helpful discussions and critical reading of the manuscript. Dr. Nishinaga is particularly appreciated for his daily discussions and advices.

Thanks are due to Dr. Charles B. Duke at University of Illinois ( Now in Xerox Co., J.C. Wilson Center for Technology, New York ) for his constant interest in this work and advices. Thanks are also due to Dr. Hiroshi Hasegawa and Dr. Kunihiro Kanda in Kyoto University for their helpful discussions and valuable suggestions.

He is deeply grateful for the conveniences and kindness of Professor Yoshika Masuda and his collaborators in the Low Temperature Laboratory of this university.

He is indebted to Drs. Nobuyuki Kobayashi, Teruyoshi Mizutani, Masahiro Kakehi and Toshiyuki Ido for their daily discussions and advices.

He is particularly grateful to Professor Noriaki Sato for his conveniences and advices in preparing the manuscript. He is also grateful to Miss Hisae Yoshida for her excellent job in tracing the figures.

This work was done in Arizumi Lab., Faculty of Engineering, Nagoya University. The numerical calculations were performed with the aid of FACOM 230-60 at Data Processing Center of Kyoto University and Computation Center of Nagoya University.

## REFERENCES

1. J.R. Oppenheimer : Phys. Rev. 31 (1928) 66.
2. Э.В. ШПОЛЬСКИЙ : АТОМНАЯ ФИЗИКА  
「原子物理学」 ( 商工出版, 1951 )
3. C. Zener : Proc. Roy. Soc. 145 (1934) 523.
4. M.S. Tyagi : Solid State Electronics 11 (1968) 99.
5. L. Esaki : Phys. Rev. 109 (1957) 603.
6. E.O. Kane : J. Phys. Chem. Solids 12 (1959) 181,  
J. appl. Phys. 32 (1961) 83.
7. L.V. Keldysh : Soviet Physics, JETP 6 (1958) 763.
8. W.A. Harrison : Phys. Rev. 123 (1961) 85.
9. D.R. Fredkin and G.H. Wannier : Phys. Rev. 128 (1962) 2054.
10. J.L. Moll : Physics of Semiconductors ( McGraw-Hill Book  
Co., New York, 1964 ).
11. W. Franz : Handbuch der Physik ed. S. Flügge ( Springer  
Verlag, Berlin, 1956) vol.17.
12. L.I. Schiff : Quantum Mechanics ( McGraw-Hill Book Co.,  
New York, 1955 ) 2nd edition.
13. A.G. Chynoweth, W.L. Feldman and R.A. Logan : Phys. Rev.  
121 (1961) 684.
14. D. Meyerhofer, G.A. Brown and H.S. Sommers : Phys. Rev.  
126 (1962) 1329.
15. J.J. Tiemann and H. Fritzsche : Phys. Rev. 132 (1963) 2506.
16. H. Roth, W. Bernard and W.D. Straub : Phys. Rev. 145  
(1966) 667.
17. N. Holonyak, I.A. Lesk, R.N. Hall, J.J. Tiemann and  
H. Ehrenreich : Phys. Rev. Letters 3 (1959) 167.
18. R.T. Shuey : Phys. Rev. 139 (1965) 1675.
19. W.P. Dumke, P.B. Miller and R.R. Haering : Chem. Solids  
23 (1962) 501.

20. L. Kleinman : Phys. Rev. 140 (1965) A637.
21. R.T. Payne : Phys. Rev. 139 (1965) A570, 154 (1967) A730.
22. H. Fritzsche and J.J. Tiemann : Phys. Rev. 139 (1965) A920.
23. A.D. Brailsford and L.C. Davis : Phys. Rev. B2 (1970) 1708.
24. L.C. Davis : Phys. Rev. B2 (1970) 1714.
25. L. Esaki : Proc. Intern. Conf. Physics of Semiconductors,  
Kyoto (1966) 589.
26. J.W. Conley, C.B. Duke, G.D. Mahan and J.J. Tiemann :  
Phys. Rev. 150 (1966) 446.
27. J.W. Conley and G.D. Mahan : Phys. Rev. 161 (1967) 681.
28. G.D. Mahan and J.W. Conley : Appl. Phys. Letters 13  
(1967) 29.
29. The results by Mahan and Conley were criticized later :  
F.A. Padovani and R. Stratton : Appl. Phys. Letters  
13 (1968) 167.
30. P.W. Anderson : Phys. Rev. Letters 17 (1966) 95.
31. J.A. Appelbaum : Phys. Rev. Letters 17 (1966) 91.
32. J.A. Appelbaum : Phys. Rev. 154 (1967) 663, 160 (1967) 554.
33. J.A. Appelbaum and W.F. Brinkman : Phys. Rev. 183 (1969)  
553, 186 (1969) 464.
34. R.N. Hall, J.H. Racett and H. Ehrenreich : Phys. Rev.  
Letters 4 (1960) 456.
35. E.L. Wolf and D.L. Losee : Phys. Rev. B2 (1970) 3660,  
Solid State Comm. 7 (1969) 665.
36. D.L. Losee and E.L. Wolf : Phys. Rev. Letters 26 (1971)  
1021.
37. A.J. Bennett, C.B. Duke and S.D. Silverstein : Phys.  
Rev. 176 (1968) 969.
38. A.M. Andrews, H.W. Korb, N. Holonyak Jr., C.B. Duke and  
G.G. Kleiman : Phys. Rev. B5 (1971) 2273.
39. C.B. Duke, G.G. Kleiman and T.E. Stakelon : in preprint.
40. I. Gieaver : Phys. Rev. 122 (1961) 1101.
41. C.B. Duke : Tunneling in Solids ( Academic Press, New York,  
1969 ).
42. R. Kubo : J. Phys. Soc. Japan 12 (1957) 570.



43. A.A. Abrikosov, L.P. Gorkov and I.E. Dzyaloshinski :  
Method of Quantum Field Theory in Statistical Physics  
( Prentice Hall, New York, 1963 ).
44. E.L. Wolf : Phys. Rev. Letters 20 (1968) 204.
45. C.B. Duke : Phys. Rev. 186 (1969) 588.
46. C.B. Duke and G.G. Kleiman : preprint.
47. J. Bardeen : Phys. Rev. Letters 6 (1961) 57, 9 (1962) 147.
48. M.H. Cohen, L.M. Falicov and J.C. Phillips : Phys. Rev.  
Letters 8 (1962) 316.
49. Tunneling Phenomena in Solids ed. E. Burstein and  
S. Lundqvist ( Plenum Press, New York, 1969 ).
50. Superconductivity ed. R.D. Parks ( Marcel Dekker Inc.,  
New York, 1969 ).
51. The term band is utterly different from that due to the  
periodicity of the crystal, and it means only a  
continuous energy spectrum. See Ref.54.
52. The electronic state may be described by some linear combination  
of the atomic states as the case of a molecule.  
J.C. Slater : Quantum Theory of Molecules and Solids  
( McGraw Hill Book Co., New York, 1963 ) vol.1 .
53. N.F. Mott : Canadian J. of Physics 34 (1956) 1354.
54. J.M. Ziman : Principle of the Theory of Solids ( Cambridge Univ.  
Press, 1964 ).
55. Y. Ando and Y. Uemura : J. Phys. Soc. Japan 30 (1971) 632.
56. V.I. Fistul : Heavily Doped Semiconductors ( Plenum Press,  
New York, 1969 ).
57. T.P. Brody : J. appl. Phys. 33 (1962) 100.
58. R.A. Logan and A.G. Chynoweth : Phys. Rev. 131 (1963) 89.
59. Semiconducttori ed. R.A. Smith ( Academic Press, New York, 1963 )
60. W. Kohn : Solid State Physics ed. F. Seitz and D. Turnbull  
( Academic Press, New York, 1957 ) vol. 5.
61. C. Kittel : Quantum Theory of Solids ( John Wiley and Sons, Inc.,  
New York, 1963 ).
62. V.L. Bonch-Bruевич : Semiconductors and Semimetals ed. R.K. Willardson  
and A.C. Beer ( Academic Press, New York, 1966 ) vol. 1.

63. P. Soven : Phys. Rev. 156 (1967) 809.
64. C. Domb, A.A. Maradudin, E.W. Montroll and G.H. Weiss :  
Phys. Rev. 115 (1959) 18, 24.
65. M. Lax and J.C. Phillips : Phys. Rev. 110 (1958) 41.
66. T. Matsubara and Y. Toyozawa : Prog. theor. Phys. 26 (1961) 739.
67. T. Matsubara and T. Kaneyoshi : Prog. theor. Phys. 36 (1966) 695,  
40 (1968) 1257.
68. F. Yonezawa : Prog. theor. Phys. 31 (1964) 357.
69. F. Yonezawa and T. Matsubara : Prog. theor. Phys. 35 (1966) 357, 759.
70. H. Hasegawa and M. Nakamura : J. Phys. Soc. Japan 26 (1969) 1362.
71. B.I. Halperin and M. Lax : Phys. Rev. 148 (1966) 722, 153 (1967) 802.
72. H. Fritzsche : J. Phys. Chem. Solids 6 (1958) 69.
73. W. Sasaki : Review at the symposium on Impurity Conduction held at the  
Institute for Solid State Physics, University of Tokyo (1968).
74. K. Morigaki : Solid State Physics ( Science Press, Tokyo ) 3 (1968) 55.
75. M.N. Alexander and D.F. Holcomb : Review of Modern Physics 40 (1968)  
815.
76. W. Sasaki : Proc. Intern. Conf. Physics of Semiconductors, Kyoto (1966)  
543.
77. J. Kondo : Solid State Physics ed. F. Seitz, D. Turnbull and  
H. Ehrenreich ( Academic Press, New York, 1969 ) vol. 23.
78. Y. Toyozawa : J. Phys. Soc. Japan 17 (1962) 986.
79. H. Miyazawa and H. Ikoma : J. Phys. Soc. Japan 23 (1967) 290.
80. H. Shiba, K. Kanda, H. Hasegawa and H. Fukuyama : J. Phys. Soc.  
Japan 30 (1971) 972.
81. V.L. Bonch-Bruевич : Soviet Physics-Solid State 4 (1963) 1953.
82. E. Yamada and T. Kurosawa : Proc. Intern. Conf. Physics of  
Semiconductors, Moscow (1968) 805.
83. M.H. Cohen, H. Fritzsche and S. Ovshinsky : Phys. Rev. Letters 22  
(1969) 1065.
84. K. Morigaki and F. Yonezawa : Solid State Physics ( Science Press,  
Tokyo ) 7 (1972) 183.
85. The term localized has not yet been confirmed.  
P. Lloyed : J. Phys. C 2 (1969) 1717,  
D.J. Thouless : J. Phys. C 3 (1970) 1559.
86. C. Haas : Phys. Rev. 125 (1962) 1965.

87. J.I. Pankov and P. Aigrain : Phys. Rev. 126 (1962) 956.
88. B. Tuck : J. Phys. Chem. Solids 29 (1968) 615.
89. Y. Takeuchi and H. Funada : J. Phys. Soc. Japan 20 (1965) 1854.
90. R.T. Shuey : Phys. Rev. 137 (1965) A1268.
91. C.B. Duke : Tunneling Phenomena in Solids Ref. 49.
92. J. Shewchun : Solid State Electronics 10 (1967) 1165.
93. A. Waxman, J. Shewchun and G. Warfield : Solid State Electronics 10 (1967) 1187.
94. In this sense the theory of tunneling is consist of the lowest order approximation. The renormalization of the states due to tunneling is therefore neglected, which will have a role in case of inelastic tunneling because of the non-local nature of scattering.
95. D. Bohm : Quantum Theory ( Prentice Hall, New York, 1951 ).
96. J. Callaway : Energy Band Theory ( Academic Press, New York, 1964 ).
97. F.W.J. Oliver : Handbook of Mathematical Functions ed. M. Abramowitz and I.A. Stegun ( Dover Pub., Inc., New York, 1965 ) p.355.
98. D.J. BenDaniel and C.B. Duke : Phys. Rev. 152 (1966) 683.
99. J.C.P. Miller : Handbook of Mathematical Functions ed. M. Abramowitz and I.A. Stegun ( Dover Pub., Inc., New York, 1965 ) p.685.
100. 寺沢 寛一 : 「 数学 概 論 」 ( 岩 波 書 店 , 1954 ).
101. If we are interested in the band edge of the valence band, we will get a similar formula to Eq.(2-67) for the energy measured from the top of the valence band.
102. T. Arizumi, A. Yoshida and N. Sawaki : Proc. Intern. Conf. Physics of Semiconductors, Moscow (1968) 108.
103. T. Arizumi, A. Yoshida and N. Sawaki : J. J. appl. Phys. 8 (1969) 700.
104. P.A. Wolff : Phys. Rev. 126 (1962) 405.
105. L.S. Rodberg and R.M. Thaler : Introduction to the Quantum Theory of Scattering ( Academic Press, New York, 1967 ).
106. P.A.M. Dirac : The Principles of Quantum Mechanics ( Oxford Univ. Press, 1958 ) 4th edition.
107. J.M. Ziman : Elements of Advanced Quantum Theory ( Cambridge Univ. Press, 1969 ).
108. S. Raimes : Many Electron Theory ( North-Holland Pub. Co., 1972 ).
109. S.F. Edwards : Phil. Mag. 3 (1958) 1020.

110. T.H. Ning and C.T. Sah : Phys. Rev. B4 (1971) 3468, 3482.
111. J.W. Blaker and R. Harris : J. Phys. C 4 (1971) 569.
112. M. Saitoh, H. Fukuyama, Y. Uemura and H. Shiba : J. Phys. Soc. Japan 27 (1969) 26.
113. N. Sawaki, A. Yoshida and T. Arizumi : J. Phys. Soc. Japan 30 (1971) 1007.
114. H. Hasegawa : private communication.
115. J. Lambe and R.C. Jaklevic : Phys. Rev. 165 (1968) 821.
116. D.J. Scalapino and S.M. Marcus : Phys. Rev Letters 18 (1967) 459.
117. W. Salaneck, Y. Sawada, E. Burstein and M. Nelson : Phys. Rev. Letters 20 (1968) 1097.
118. C.B. Duke, G.G. Kleiman, A.M. Andrews, R.D. Burnham, N. Holonyak Jr. and H.W. Korb : Proc. Intern. Conf. Physics of Semiconductors, Cambridge (1970) 856.
119. Actually the inequality doesn't hold generally. In the case of tunneling, the value of the integrand in Eq.(3-49) for large  $\epsilon_k$  can be neglected because of the exponential factor. This approximation is confirmed by the nature of the spectral function, i.e., it has a maximum near  $\epsilon_k = E - \text{Re} \Sigma$ . See Ref. 62.
120. T.H. Geigalle : Semiconductors ed. N.B. Hannay ( Reinhold Pub. Co., New York, 1959 ).
121. J.V. Morgan and E.O. Kane : Phys. Rev. Letters 3 (1959) 466.
122. P.J. Price and J.M. Radcliffe : I.B.M. J. Res. Develop. 3 (1959) 364.
123. W.N. Carr : J. appl. Phys. 34 (1963) 2467.
124. C. Constantinescu and I. Midvich : phys. stat. solidi. 8 (1965) 261.
125. H. Fritzsche and J.J. Tiemann : Phys. Rev. 130 (1963) 617.
126. W.R. Patterson and J. Shewchun : Rev. Sci. Instrum. 35 (1964) 1704.
127. B. Lax and J.G. Mavroids : Solid State Physics ed. F. Seitz and D. Turnbull ( Academic Press, New York, 1960 ) vol. 11.
128. R.J. Bate : J. appl. Phys. 33 (1962) 26.
129. J.C. Slater : Quantum Theory of Molecules and Solids ( McGraw-Hill Book Co., New York, 1967 ) vol. 3.
130. H. Hasegawa : private communication.
131. J.R. Schrieffer : Many Body Problem ed. R. Kubo ( Syōkabō, Tokyo, 1966 ).
132. A. Zawadowski : Phys. Rev. 163 (1967) 341.

133. R.T. Payne : Phys. Rev. Letters 21 (1968) 284.
134. R.E. Prange : Phys. Rev. 131 (1963) 1083.
135. C.B. Duke and M.J. Rice : Phys. Rev. 181 (1969) 733.
136. H. Fukuyama, M. Saitoh, Y. Uemura and H. Shiba : J. Phys. Soc. Japan 28 (1970) 842.
137. M. Saitoh : J. Phys. Soc. Japan 29 (1970) 1470.
138. N. Sawaki : unpublished. See Ref. 70.
139. T. Yamanouchi : J. Phys. Soc. Japan 18 (1963) 1775.
140. T. Matsubara and T. Kaneyoshi : Prog. theor. Phys. 40 (1968) 1257.
141. H. Fukuyama : Prog. theor. Phys. 42 (1969) 1284.
142. T. Kaneyoshi : J. Phys. C 5 (1972) 247.
143. K. Kanda and Y. Onodera : annual meeting of the Phys. Soc. Japan, April, 1971.
144. K. Kanda and H. Hasegawa : private communication.
145. Y. Toyozawa : private communication.
146. E.O. Kane : Phys. Rev. 131 (1963) 79.
147. F.C. Lackmann and M. Cyrot : J. Phys. C 5 (1972) 209.
148. This nature of Sb atoms seems to be closely related to the lower solubility in a germanium single crystal. See Ref. 56.
149. M. Cuevas and H. Fritzsche : Phys. Rev. 137 (1965) A1847.
150. M. Cuevas and H. Fritzsche : Phys. Rev. 139 (1965) A1628.
151. H. Fritzsche : Phys. Rev. 125 (1962) 1560.
152. H. Kaplan : J. Phys. Chem. Solids 24 (1963) 1593.
153. G.A. Peterson : Proc. Intern. Conf. Physics of Semiconductors, Paris, (1964) 771.
154. W. Paul : Proc. Intern. Conf. Physics of Semiconductors, Moscow, (1968) 16.
155. M. Lax and B.I. Halperin : Proc. Intern. Conf. Physics of Semiconductors, Kyoto, (1966) 218.
156. K.F. Freed and M.H. Cohen : Phys. Rev. B3 (1971) 3400.
157. N.F. Mott : Phil. Mag. 17 (1968) 1259.
158. S.H. Koenig : Proc. Intern. Conf. Physics of Semiconductors, Exeter, (1962) 5.
159. H. Yamada and S. Takada : Prog. theor. Phys. 48 (1972) 1828.
160. J. Kondo : Prog. theor. Phys. 32 (1964) 37.
161. J. Solym and A. Zawadowski : Phys. Kondens. Materie 7 (1968) 325,342.

- 162. J.J. Tiemann and H. Fritzsche : Phys. Rev. 137 (1965) A1910.
- 163. H. Brooks : Advances in Electrons and Electron Physics ( Academic Press, New York, 1955 ) vol. 17.
- 164. N. Sawaki and T. Arizumi : J. Phys. Soc. Japan 33 (1972) 725.
- 165. Y. Nagaoka : Phys. Rev. 138 (1965) 49.

## LIST OF REPORTS

- 1) Density of States and Band Tail of (000) and (100) valleys of Heavily Doped Semiconductors ;  
T. Arizumi, A. Yoshida and N. Sawaki : Proc. Intern. Conf. Physics of Semiconductors, Moscow (1968) p. 108.
- 2) Uniaxial Stress Effect on (000) and (100) Conduction Band Minima of Germanium ;  
T. Arizumi, A. Yoshida and N. Sawaki : Japan J. appl. Phys. Vol. 8 (1969) p. 700.
- 3) Uniaxial Stress Effect on Subsidiary Band Minima of GaSb from Zero Bias Conductance Anomaly ;  
N. Sawaki, A. Yoshida and T. Arizumi : Japan J. appl. Phys. Vol. 9 (1970) p. 922.
- 4) Tunneling through Band Tail States ;  
N. Sawaki, A. Yoshida and T. Arizumi : J. Phys. Soc. Japan Vol. 30 (1971) p. 1007.
- 5) Magnetic Scattering in Germanium Tunnel Diode ;  
N. Sawaki and T. Arizumi : J. Phys. Soc. Japan Vol. 33 (1972) p. 725.
- 6) Theory of Tunneling into Impurity Band ;  
N. Sawaki and T. Arizumi : to be published in J. Phys. Soc. Japan Vol. 35 (1973) No. 3.
- 7) Tunneling Spectroscopic Study of Impurity Band of (000) valley of Germanium ;  
N. Sawaki, A. Yoshida and T. Arizumi : submitted to J. Phys. Soc. Japan.